

# Commercial glass strengthening and safety technologies: lessons learned and yet to be learned

Guglielmo Macrelli,<sup>1</sup> Arun K. Varshneya,<sup>2,\*</sup> Stefan Karlsson<sup>3</sup> & John C. Mauro<sup>4</sup>

<sup>1</sup> Isoclima SpA, R&D Department, Via A.Volta 14, 35042 Este (PD), Italy

<sup>2</sup> Saxon Glass Technologies, Inc. and Alfred University, Alfred, NY, USA

<sup>3</sup> RISE Research Institutes of Sweden AB, Department of Materials and Surface Design, Vejdes plats 3, 352 52 Växjö, Sweden

<sup>4</sup> Department of Materials Science and Engineering, The Pennsylvania State University, University Park, PA 16802, USA

Manuscript received 14 December 2023

Revised version received 1 June 2024

Accepted 3 June 2024

---

*This is the fourth in this series of “Lessons Learned and Yet to be Learned” on topics related to glass strength.<sup>(1–3)</sup> In this paper we pick up the topic of stronger glass products from our earlier publication<sup>(2)</sup> and expand to discussing commercial technologies. Included in this discussion are a brief historical perspective of the initial technologies and update to newer technologies with the aim to obtain faster production rates that focus on lightweight glass products and a sustainable future with respect to resource conservation, reduced energy consumption and reduced CO<sub>2</sub> emissions. Also included are glass products which focus on safety mostly and less on overall strength.*

---

## 1. Introduction: historical perspective

Glass is a material with many appealing properties such as transparency or translucency which, together with chemical stability, are the main functional characteristics considered in their use and applications.<sup>(4,5)</sup> Beside these appealing features, brittleness is the most critical drawback for glass.<sup>(2)</sup> Glass articles usually break quite suddenly without prior indication of an imminent failure. In theory, brittleness implies that there is no measurable reduction of cross-sectional area at the point of fracture. Unlike metals, glass does not display any yield phenomenon<sup>(6)</sup> or ductility at a macroscopic level where the applied stress reaches a “yield strength” and causes plastic deformation until fracture. However, it is well known that the region around indentation and abrasion in glass does show ductility and plastic deformations on a microscopic and, likely, on a nanoscopic level.<sup>(3,7)</sup> When thinking about stronger glass products, one may recall “unbreakable glass”. Articles with such a high strength that can be considered “unbreakable” are the subject of old myths and legends. Traces<sup>(8–10)</sup> can be found in ancient literature since 63 BCE of a legendary malleable glass named “*vitrum flexile*” (in Latin language, meaning flexible glass). This was a material, supposedly transparent or translucent, that can be worked

with a hammer like a metal. This legend did not stop there but survived through the centuries in different forms, spreading geographically in Persia<sup>(11)</sup> and Spain<sup>(12)</sup> through France<sup>(13)</sup> and reported in alchemic recipes<sup>(13,14)</sup> translated to English<sup>(15)</sup> and also mentioned in the famous treatise of Antonio Neri.<sup>(16)</sup> The fate of the ancient artisans who allegedly discovered this “*vitrum flexile*” did not turn out to be pleasant;<sup>(9,10,12)</sup> they were put to death, or imprisoned for life and their workshops destroyed. Additionally, if we look to the alchemic recipe of the “malleable glass” some critical issues can be noted suggesting not to try the experiment under uncontrolled condition as it requires sublimation of mercury that can have dramatic consequences to the health. It is interesting to note that, even in the ancient literature, the main feature considered for the “*vitrum flexile*” was not its “unbreakability” but that it was possible to work and repair glass with a hammer like a metal. This indicates a certain wisdom of the ancients that should be suggested also to contemporary engineers in glass structural design whereas it is not only the exceptionally high strength of glass articles to be considered but, additionally, their capability to handle high stress conditions by molecular dissipation mechanisms. The stories of unbreakable glass do not end there but the history reveals several other stories of such kind. Petronius’s tale from AD 66<sup>(10,17)</sup> that involves a story of a craftsman who made a bowl of unbreakable glass

---

\*Corresponding author. Email varshneya@alfred.edu  
DOI: [10.13036/17533546.65.3.06](https://doi.org/10.13036/17533546.65.3.06)

(*phialam vitream quae non frangebatur*), also referred to as “*vitrum flexile*”. The unbreakable bowl amazed the emperor when it remained intact after being dropped on the floor. The report made some modern commentators to have claimed that Petronius’s tale is evidence for the Roman development of thermal tempering techniques<sup>(17–19)</sup> of placing the outside surface of glass in a state of large compression. The story of Aleardino’s Glass from the 13th century is another legendary story, originating from the fact that a silver mounted drinking glass miraculously remained intact after being thrown to the ground by the heretical knight Aleardino.<sup>(17)</sup>

Since then, significant steps forward to both the understanding of the mechanism of glass breakage as well as towards stronger glass products have been taken. Prince Rupert’s drops are famous for a practical phenomenon of thermal tempering of glass; they are also known as the Batavian, Prussian or Dutch tears.<sup>(20,21)</sup> The inventor of them was certainly not Prince Rupert, though he was instrumental in bringing the drops to Britain in 1660. The following reports of the Royal Society refer to the drops and describe experiments performed including observations by Hooke.<sup>(22,23)</sup> Again, there are suggestions that the drops have been known to glassmakers since the Roman Empire<sup>(24)</sup> but the invention is sometimes attributed to Cornelis Drebbel.<sup>(25)</sup> Verifiable accounts have been found as early as 1625 in Mecklenburg in North Germany,<sup>(26)</sup> thereof the various names of the drops. The first patents on thermal strengthening came in the 1870s with de la Bastie in 1874<sup>(27,28)</sup> involving quenching of hot glass in mixtures of oils and greases.<sup>(29)</sup> Siemens 1875<sup>(30,31)</sup> had a more industrial approach and combined forming the glass by pressing cold metal or clay.<sup>(29)</sup> The development continued<sup>(32,33)</sup> whereas a more-or-less complete tempering process was first patented in 1934 by Seiden.<sup>(28,34)</sup> The scientific understanding of thermal strengthening of glass has a lot in common with the scientific understanding of annealing of glass where notable work by Adams & Williamson,<sup>(35)</sup> Bartenev,<sup>(36)</sup> Acloque,<sup>(37)</sup> Gardon & Narayanaswamy<sup>(38)</sup> and Guillemet<sup>(39)</sup> can be mentioned. In the 1970s the development of thermal strengthening in liquid medium as well as solid contact tempering was founded.<sup>(40)</sup>

The development of stronger commercial glass products has a lot in common with thermal shock which led to the development of glasses and glass-ceramics with low thermal expansion coefficient. A famous example is the invention of borosilicate glass which normally is credited to Schott<sup>(41,42)</sup> in the 1880s even though both Faraday<sup>(43)</sup> and Harcourt<sup>(44)</sup> made experiments with boron oxide in silicate glass previously. Borosilicate glasses not only have a thermal expansion of  $\sim 3 \times 10^{-7}/\text{K}$  but also significantly better chemical resistance than the conventional soda-lime-silica composition.<sup>(45)</sup> After World War I, the

borosilicate glass Pyrex<sup>®</sup> was invented which showed improved performance in mechanical shock.<sup>(46)</sup> Schott also invented the strengthening method of overlaying a low expansion glass over a high expansion core glass,<sup>(47)</sup> an early glass composite. Continuing on composites, in 1912, the “TriPlex<sup>®</sup>” was invented in France,<sup>(48)</sup> a product which we today most commonly call laminated glass. The triplex invention was based upon previous work by Fullicks<sup>(49)</sup> and Woods.<sup>(50)</sup> The laminated glass development after the World War I, where it was used in windshields, then followed with the development of the automotive industry.<sup>(51–53)</sup> In 1953 Stookey<sup>(54)</sup> invented Pyroceram<sup>®</sup>, a glass-ceramic material with a very low coefficient of thermal expansion ( $\sim 3 \times 10^{-7}/\text{K}$ ). It, for instance, led to the development of oven-resistant cookware Corningware.<sup>(54)</sup> The success of Pyroceram<sup>®</sup> led to the Corning venture on strengthening of glass, “*Project Muscle*”, that will again be mentioned in the next section). [Footnote: There are some unverified accounts of the invention of glass-ceramics by German scientists for use in missile cones during World War II].

Similar to the relation with thermal shock, the development of stronger glass products also has a lot in common with surface chemistry. In the early industrial development of glass manufacturing was one of the issues chemical durability,<sup>(45)</sup> especially for glass containers<sup>(55)</sup> eventually led to the discovery of dealcalization of glass surfaces<sup>(56–58)</sup> where acidic gases or liquids at elevated temperatures reacts with the  $\text{Na}^+$  ions in the glass surface leaving a dealcalized surface and a glass that is strengthened with the same principle as overlaying a low expansion glass over a high expansion glass.<sup>(47,59)</sup> Kistler, an American chemist and inventor of aerogel,<sup>(60)</sup> formulated a process based on others’ work on manipulating the surface chemistry.<sup>(61–63)</sup> The process today is known as chemical strengthening (independently invented by Acloque & Tochon<sup>(64)</sup>). Corning and the “*Project Muscle*” picked this up and advanced it further<sup>(65,66)</sup> resulting in the product brand Chemcor<sup>(67)</sup> which later led to the product brand “Superfest”<sup>(68)</sup> in the German Democratic Republic (GDR).

In today’s society, there is a huge spread of different commercial glass products where strength is an important property, e.g. in structural applications ranging from architectural, transportation, consumer electronics, and pharmaceutical. In these applications windows or articles made of glass components are designed and exposed to critical situations like: tornadoes, hurricane-force winds, high speed impacts (hail stones and other stones), environmental critical conditions, shocks, surface scratch and abrasion. In some applications, the failure of the integrity of a glass component may result in a highly risky situation that can put human lives in danger such as during administration of epinephrine from an autoinjector during potential anaphylaxis shock from severe allergens

such as bee stings, peanuts, and shell fish and due to birds hitting the cockpit windshields of aircrafts while in flight. Additionally, there is increased emphasis on sustainability such as resource conservation, energy conservation and reduced CO<sub>2</sub> emissions (“green” processing). There is intense global effort to reduce the weight of glass products and to use less energy for making them. In this paper, we briefly review the basic science of glass strength to discuss the various common commercialized processes to manufacture stronger glass products from a high level view. We have also taken a historical perspective to see if there are any lessons learned.

## 2. Glass strength

Strength implies the magnitude of an applied stress to fracture. Since stress is a second rank tensor, a generalized stress can be considered to be composed of a hydrostatic component which changes the volume and not the shape, and a deviatoric (or pure shear) component which changes only the shape but not the volume. Glass breaks only when a tensile component of the stress field exceeds the strength of the atomic bonds. Under pure hydrostatic compression, the network densifies; a value of strength under pure compression is not known. From a basic science point of view, the energy to be applied to a glass product to cause a fracture of atomic bonds must at least equal the surface energy of the two freshly created surfaces (the release argument). Thus, according to Orowan,<sup>(69)</sup> the theoretical strength  $\sigma_m$  of a *flawless* brittle solid is given by:

$$\sigma_m = \sqrt{\frac{\gamma_f E}{a_0}} \quad (1)$$

where  $E$  is the Young’s modulus,  $a_0$  is atomic separation and  $\gamma_f$  is the fracture surface energy. Assuming  $E=70$  GPa,  $a_0=0.2$  nm and  $\gamma_f=3.5$  J/m<sup>2</sup>, one obtains  $\sigma_m=35$  GPa.

Significant steps towards understanding the mechanisms of glass breakage has been performed by following the principles of fracture mechanics<sup>(70)</sup> involving the growth or propagation of flaws. Flaws can be intrinsic or extrinsic. Intrinsic flaws are those that are created in the glass network presumably by cavitation during glass forming as suggested by Ito & Taniguchi.<sup>(71)</sup> One may imagine that a random network of atoms may house large randomly sized interstitial spaces due to the forming operations. It can also be argued that intrinsic flaws cause the strength of the glass to decrease from a theoretical value of ~35 GPa down to 12–14 GPa maximum observed to date.<sup>(72)</sup> A continuous random network should have four independent yield strengths: for hydrostatic compression, hydrostatic dilation, planar shear and twist shear. The stress field around the indent or abrasion is likely controlled by the yield

strength for hydrostatic compression and the planar shear yield strength. For fracture at the site of an extrinsic flaw, generally a surface flaw created due to handling of the glass product in contact with just about anything, either the applied stress is amplified at the flaw’s tip to exceed the bonding strength of the glass components, or a sub-critical crack growth enhanced by the reaction of water at the crack tip, frequently called stress corrosion<sup>(73)</sup> or static fatigue occurs. The former argument, due to Inglis,<sup>(74)</sup> gives the strength of a *flawed* brittle solid as:

$$\sigma_f = \sqrt{\frac{\gamma_f E}{2c}} \quad (2)$$

where  $c$  is the length of an assumed semi-elliptical flaw drilled into the glass surface and the theoretical strength has been rewritten as a practical strength  $\sigma_f$ . A  $c=50$   $\mu\text{m}$  flaw can reduce the observed strength down to 50 MPa which is a usual value for the breaking strength of glass products. The argument of energy requirement to cause a flaw to grow was advanced by Griffith<sup>(75)</sup> who, then, obtained an expression similar to Equation (2) but with slight difference of constants:

$$\sigma_f = \sqrt{\frac{2\gamma_f E}{\pi c}} \quad (3)$$

Despite their lengths, the width of a flaw can be of atomic dimensions, hence these flaws are difficult to be observed even by the highest resolution electron microscope. Strengthening of glass products must, therefore, address these extrinsically created “Griffith flaws”.

Irwin<sup>(76)</sup> advanced the concept of flaw growth to assign  $\sigma_a[\pi c]^{1/2}=[2\gamma_f E]^{1/2}=K_I$ =stress intensity factor at the applied stress. When  $c \rightarrow c^*$ ,  $K_I \rightarrow K_{Ic}$ , the critical stress intensity factor, also called “fracture toughness” and  $\sigma_a \rightarrow \sigma_f$ . Research pioneered by Wiederhorn and his colleagues at the National Bureau of Standards (now the National Institute for Standards and Technology) supports this view.<sup>(77)</sup> Particularly the effect of humidity on fracture strength is now well understood. Their key result is shown in Figure 3 from Ref. 2. Essentially, the sub-critical crack propagation velocity increases with the magnitude of the applied stress intensity factor  $K_I$  and the level of humidity.

The crack grows upon application of a  $K_I$ , which with a small time increment yields a larger  $K_I$ , hence, a larger crack velocity. The state of the glass thus gradually moves up the curve until  $c \rightarrow c^*$  and  $K_I \rightarrow K_{Ic}$ . Fracture is imminent at that point. Glass strength is the highest under inert N<sub>2</sub> atmosphere, particularly at low temperatures. A final note here: there is no such thing as an *unbreakable glass*. In fact there is no such thing as an unbreakable anything. All we can try to achieve is a reduction of the fracture probability.

The overall basic science of fracture mechanics discussed above guides us into the practical develop-

ment towards stronger glass products:

- (1) Management of glass product geometry
- (2) Management of flaws
- (3) Management of the environment (sub-critical crack growth due to stress-assisted corrosion of the flaw tip).
- (4) Management of applied tension
- (5) Management of glass composition to optimize the strength
- (6) Management of energy absorption
- (7) Testing methods

Each of these topics is briefly reviewed next.

### 3. Commercial glass strengthening technologies

In all our interacting experiences with glass we expect that the glass elements will not fail due to service loads to which it may be exposed. When the failure of a product potentially has an adverse consequence putting human lives in danger or the integrity of structures and goods a suitable design activity is a necessary step taking in due consideration the materials properties and the type and level of service loads. In design there can be found two elements of consideration:

- (A) Design products in such a way that they do not fail under a defined load situation
- (B) Design products in such a way that even if they fail, the failure does not provoke damages to people or goods.

Taking a similar route from thermodynamics, design of type (A) is a kind of “reversible” situation where the product can be exposed to service loads many times and it is expected to work reversibly at any exposure without failure. Design of type (B) is a kind of “irreversible” situation where we admit a controlled failure of the product providing safety and security requirements but requesting a product replacement. Examples of type (A) are: the wind resistance of the glazing pane of a window or the resistance of a glazing floor to withstand the load of people walking on it. Examples of type (B) are the bullet resistance of an armored glazing or the resistance of an external glazing to a burglary attack. The design of stronger glass product followed two lines of thought: increase the strength of glass in terms of characteristic breakage strength expressed as a stress value corresponding to an acceptable probability of failure or combine glass elements in composite constructions with viscoelastic polymers to overcome practical thickness limitations. Such composite is designed to be capable of absorbing energy beyond glass elements failure, and to avoid projection of sharp glass shards after glass elements failure. International regulations and standards dictate or recommend to engineers how to design and test products incorporating glass elements in order to

provide either safety and security in real applications. In most applications, the approach to glass strength based on the macroscopic mechanical behaviour that can be described by linear fracture mechanics is quite acceptable. As pointed out in previous sections this first approximation level, neglecting the nanometric dissipation yield phenomena in monolithic glass bodies, accounts well for the apparent brittle feature of glass breakage. The evolution of stronger glass products has achieved in recent times a significant level both in terms of dimensions of glass elements and in terms of availability of materials and strengthening technologies. The float process<sup>(78)</sup> has been confirmed as the most effective to provide silicate glass plates with large dimensions (jumbo size) 6 m×3.21 m that can be extended to 10–12 m in length. These huge plates, exceeding the “standard jumbo” size, can be presently strengthened either by thermal or chemical means in existing plants. In addition, bending processes of flat plates in cylindrical and Gaussian curvature open the possibility to use stronger glass products in architectural applications like facades, stairs and balustrades. This evolution is not limited to architectural applications but can be extended to transportation vehicles such as ships, cruisers or luxury yachts. The next frontier in this specific development is the extension of the float process to different silicate glass chemical compositions. Presently, both borosilicate and alkali aluminosilicate (and boroaluminosilicate) glass are manufactured by the float process. This opens the possibility to have a silicate glass with a chemical composition suitably designed for chemical strengthening in order to achieve a higher residual surface compression stress and a deeper depth of compression. The rather remarkable evolution here is to achieve thinner glass products.

The consumer electronics applications in displays for smart phones, tablets, TV and personal computers evolved from the thin aluminosilicate glass of 1 mm to the ultra-thin applications down to 30  $\mu\text{m}$  thickness. Ultra-thin glass, a glass with a thickness lower than 0.5 mm, leads to the concept of flexible glass and foldable glass.<sup>(79)</sup> Draw-down and overflow forming processes extended to widths exceeding 1m clearly indicate an evolution path that can likely flow over to applications in different markets.

#### 3.1 Management of glass product geometry

In reality, strengthening a glass product starts with optimizing the geometry against potential hazards. It is understood that, for an optimum strength performance, glass products need to be as close to a cylindrical shape as possible (if not spherical). Wall thicknesses need to be adequate in order to provide mechanical robustness (resistance to being bent by impact of other bodies, projectiles, etc.) and resistance to fracture against internal pressure. Sharp corners are

to be avoided. Re-entrant angles at the corner of the container wall and the bottom should be rounded and not sharp. Outside surfaces should be free of ridges and inscriptions. Manufacturing codes inscribed using moulds should be close to the centre of the bottom. Screw threads in the bottle mouth should not have cold glass shear marks.

### 3.2 Management of flaws

It is difficult to reduce the generation of intrinsic flaws. Perhaps application of high shearing forces on the glass during the forming operations cause generation of intrinsic flaws by “liquid fracture”. By the same token, a slower application of forming stresses can give time for the molten glass to heal itself. However, that would slow down the manufacturing speeds (which no one likes).

Extrinsic flaw population is best controlled by reduced handling: reduced contact with hard metal surfaces. The forming machines should be fitted with soft mould materials. The single most helpful process that leads to reduction of surface flaws is the application of hard (“hot-end”) and/or lubricious coatings (“cold-end”).

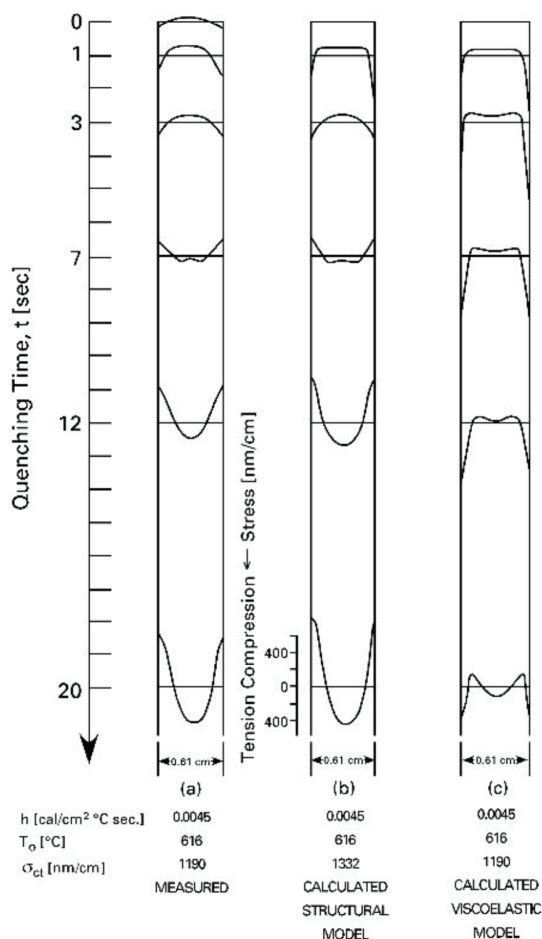


Figure 1. Cross-sectional stress distributions of a plate glass during quenching through the glass transition range. Reprinted from Narayanaswamy<sup>(86)</sup>

The foremost example of protective coatings is the hot-end coating on container glasses which has become an industry standard, after the initial pioneering work of Rawson & Turton.<sup>(80)</sup> Hot-end coatings are applied to the glass product as a spray at the entrance of the annealing lehr. Tin chloride is a usual hot-end coating candidate. Diamond-like carbon (“DLC”) and superhard coatings also provide protection against indenting objects. The technology of DLC for large glass products still needs development. The purpose of the hot-end coatings is to make the glass surface much harder to be indented, or abraded readily. Cold-end coatings, those applied on the glass product using a spray on exiting the annealing lehr, are usually soap coatings; often made as a very dilute solution of polysorbic acid in water. The purpose of the cold-end coatings is to improve the lubricity of the glass surface such that indents during transport are minimized.

The subject of flaws, hardness, indentations, abrasion and soft/hard coatings has been discussed in greater detail in a recent paper by our group.<sup>(3)</sup>

### 3.3 Management of the environment

Most commercial glass products are manufactured and handled in ordinary atmospheres and varying levels of humidity. Silanes, epoxy coatings, and thin polymeric films help to exclude the direct access of the atmospheric humidity to the glass surface. However, there really isn’t a lot of protection for traditional consumer glass product.

### 3.4 Management of applied tension

The best remedy to reduce the effect of a given applied tension is to introduce surface compression in the glass product. This technique has drawn the most attention for commercial glass products. There are three principal techniques: Thermal tempering, chemical strengthening, and overglazing.

#### 3.4.1 Thermal tempering of glass

##### 3.4.1.1 Tempering of >2 mm thick plates (air, liquid, solid contact)

The first attempts to set up theories of thermal tempering of glass and of its technological embodiment at industrial scale can be tracked back to last century between the late 1940s and early 1950s.<sup>(81–83)</sup> The applications of thermally tempered glass spread across different industries because of the superior strength and the safety breakage pattern of the thermally strengthened glass articles. The standardization of thermally tempered glass achieved an established definition for the automotive industry applications at the beginning of the 1970s.<sup>(84,85)</sup> Thermal tempering of glass products is founded in the science of permanent

stress development in glass as it cools through the glass transition. This is well explained by Varshneya & Mauro (in their Figure 3).<sup>(6)</sup> Glass products have a finite wall thickness; the key is how the various layers of the wall are cooled from above the glass transition temperature. An adequate summary statement is that the various layers of glass with an initial temperature gradient cooling through the glass transition region with varying cooling rates and at various instants of time will develop permanent stresses through the wall thickness. The first of these alludes to a “frozen” temperature gradient which results in viscoelastic development of stress (Bartenev<sup>(36)</sup>); the second to the permanent structural heterogeneity developing from the volume–temperature diagram and the last of these, brought to public attention by Gardon, is due to the “frozen fictive temperature gradient” (a “structural mechanism”) across the wall. Since the thermal expansion coefficient (more appropriately, the “thermal contraction coefficient”) for most commercial silicate glasses is usually positive, one expects to have surface compression develop in outer layers while a balancing tensile stress develops in the inner layers. Figure 1 taken from Narayanaswamy<sup>(86)</sup> elegantly shows the measured stresses (“A”) to match those calculated using the composite “structural” model (“B”) and disagree with Bartenev’s “viscoelastic” model (“C”). Note also, glass products may develop mild surface tension at early times during the cooling. Gardon & Narayanaswamy have further shown that the measured density of glass elements as a function of radial location in an unbroken plate as well as in a broken plate and stress-relieved specimen agree well with the expectations.<sup>(86,87)\*</sup>

The development of stress during cooling through glass transition has been described phenomenologically by several authors.<sup>(29,38,82,86,88–91)</sup> A grossly simplified approximate description of an assumed initial temperature distribution  $T(x,t)$  and the ending equibiaxial stress distribution  $[\sigma_{y,t}]_x$  or  $[\sigma_{z,t}]_x$  as a function of location  $x$  along the thickness ( $x=0$  at the centre of the plate) in a semi-infinite plate of thickness  $L$  shown in Figure 2) is given by

$$[\sigma_y]_x = [\sigma_z]_x = \left[ \frac{E\alpha(T_x - T_A)}{(1-\nu)} \right] \quad (4)$$

where  $T_A$  is the average temperature through the wall thickness. The thermal contraction coefficient has to be a composite value of solid state contraction coefficient plus structural contraction coefficient. If the temperature distribution were parabolic (corresponding to natural cooling), the stress distribution will also be parabolic with the magnitude of surface compression  $|\sigma_c| = 2\sigma_T$ .

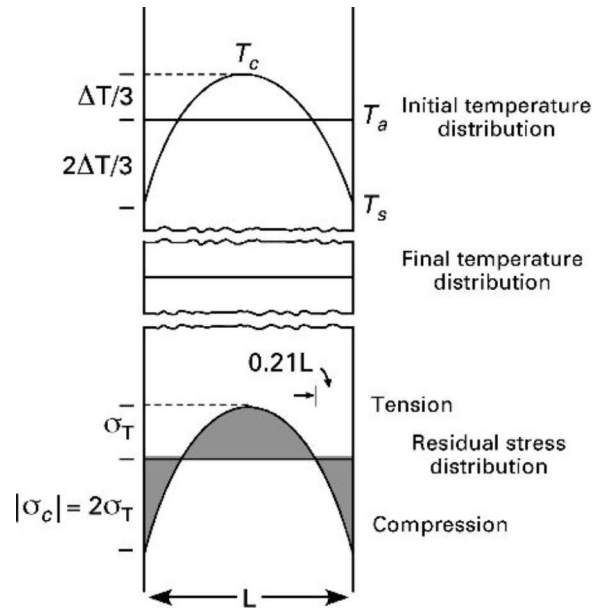


Figure 2. Principles of the parabolic stress profile distribution of tempered glass

By cooling more and more rapidly, the parabolic distribution of temperature steepens in the surface layers, becoming more and more like an error function distribution, with the result that the magnitude of surface compression may exceed two times the magnitude of interior tension. Thermal tempering technology therefore aims to develop as high a temperature gradient at the start and quenching through the glass transition at as high rate as possible. Correspondingly, thermal tempering employs quenching using gas, fluid, and solid contact, each having different heat transfer coefficients at the contact surface. Figure 3 shows that higher surface compression (measured as midplane tension termed “degree of temper”) is developed in larger wall thicknesses of the glass product. The usual 6 mm thickness glass window can be thermally tempered readily and significantly. As shown in Figure 3 below, thermal tempering of a soda–lime–silica glass can be achieved down to >2 mm thickness. Below <2 mm thickness, a large enough temperature gradient cannot be established using traditional techniques. A 100 μm or so diameter glass fibre cannot be meaningfully strengthened by the usual means of thermal tempering.

With increased emphasis on lightweighting of glass products and sustainability, technology of thermal tempering of glasses thinner than around 2 mm has drawn attention and is far more advanced, as described below.

#### 3.4.1.2 Tempering of <2 mm thin plates

The application of the thermal tempering process for both thin glasses (thickness lower than 2 mm) and for glasses with a lower linear thermal expansion coefficient has limitations. Kiefer & Lindig<sup>(92)</sup> showed

\* This portion of the text is dedicated to the memory of Dr Robert Gardon who was manager of one of the authors, AKV, in his first employment at Ford Scientific Laboratories, Dearborn MI. Although the author did not get along with him, scientific discourse must go beyond personal conflict.

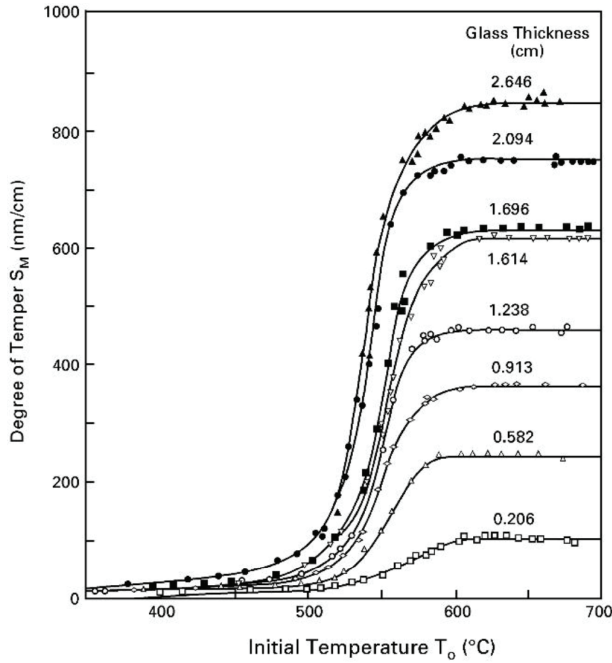


Figure 3. Degree of temper as a function of initial temperature and glass thickness

that the main limitation factor was the technology to achieve a higher heat transfer coefficient between the glass surface and the quenching medium. This was discussed by Kiefer<sup>(93)</sup> using a roughly approximated formula based on the instant freezing theory approach supported by a simplified heat transfer model:

$$\sigma_v = \frac{hX}{\lambda + hX} \frac{\alpha E}{(1 - \nu)} (T_g - T_\infty) \tag{5}$$

where:  $\alpha$  (1/K) is the linear thermal expansion coefficient of the glass,  $\lambda$  (W/mK) is the glass thermal conductivity,  $X$  (m) is the glass plate half thickness,  $E$  is the glass Young’s modulus (MPa),  $T_g$  is the glass transition temperature (K),  $T_\infty$  is the temperature of the quenching medium (K) and  $h$  (W/m<sup>2</sup>K) is the heat transfer coefficient between glass surface and quenching medium.

Although the above formula is more an approach for experimentalists than for scientific detailed modelling, it provides a useful insight to understand the problems related to thermal tempering of thin glass or low thermal expansion glasses. Detailed models of deformations and stresses in glass thermal tempering can be found in Aronen.<sup>(94)</sup> The analysis of heat transfer coefficient shall be constrained by the point that temporary tensile stress generates during quenching. As long as the glass surface temperature is above  $T_g$ , stresses, either compressive or tensile, cannot build-up. After the glass surface has reached the freezing temperature, the surface continues to cool down at a quicker rate than the glass interior and the glass interior is at a temperature above the freezing one. This condition generates a transient tensile stress in the near surface layer. It is obvious

that a condition shall be defined where the transient tensile stress does not lead to glass breakage. This is set by Kiefer,<sup>(93)</sup> again with a rough approximated practitioners formula, limiting the maximum achievable compressive stress according to Equation (6):

$$\sigma_v \leq \sigma_{BZ} + \frac{\alpha E}{(1 - \nu)} (T_A - T_g) \tag{6}$$

where  $\sigma_{BZ}$  is the maximum allowable bending strength of the annealed glass (usually around 50–60 MPa) and  $T_A$  is the maximum temperature achieved by the glass before quenching. Condition (6) defines a maximum value of the compressive stress that can be introduced by thermal tempering which depends on the maximum allowable bending strength of the annealed glass. This maximum compression value is –150 MPa for soda–lime–silica glass and –105 MPa for borosilicate glass, considering a value of  $\sigma_{BZ}$ =60 MPa for both glass types. Combining Equation (5) and Equation (6) we can evaluate in Figure 4 the thermal tempering limitations in terms of the required heat transfer coefficient  $h$  versus thickness and thermal expansion coefficient to limit of surface compression value to about –100 MPa in order to avoid glass breakage from transient tensile stress.

Values of  $h$  above 500 W/m<sup>2</sup>K are technologically unpractical using common air quenching blowing equipment. This means that the –100 MPa surface compression for borosilicate glass is almost unachievable by conventional quenching technologies. A reasonable surface compression limit compatible with conventional quenching technologies for borosilicate glass is between –50 and –70 MPa.

Table 1 reports typical values of heat transfer coefficients in different quenching implementations. The most common types of glass tempering furnaces are designed with ceramic rolls conveying systems for both heating up and quenching phases of the process and with blowing air jets for the quenching phase.

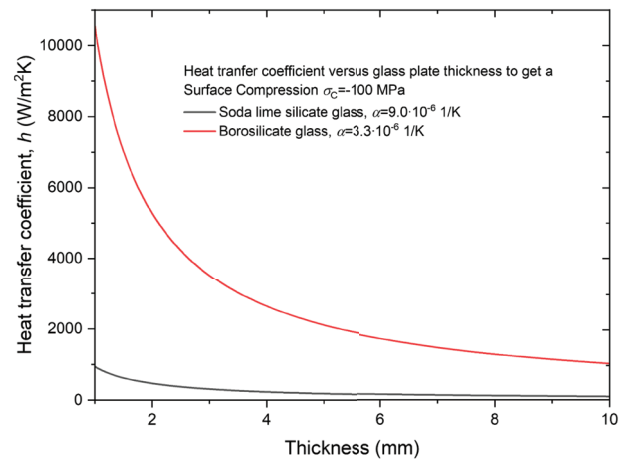


Figure 4. Required heat transfer coefficient  $h$  versus plate thickness to get a surface compression of –100 MPa for two different types of glasses: soda–lime–silica (black curve) and borosilicate (red curve) [Colour available online]

Table 1. Heat transfer coefficients for different quenching technologies in glass thermal tempering

Thermal tempering technology	Heat transfer coefficient $h$ (W/m <sup>2</sup> K)
Blowing air jets against glass surfaces (values depend on air pressure and nozzles design)	100–300
Ceramic rolls conveying technology	
Blowing air jets against glass surfaces (values depend on air pressure and nozzles design)	100–500
Cushion air conveying technology	
Mineral oils	200–600
Mineral oils with CCl <sub>4</sub>	400–1600
Spraying with air/water	500–1500
Oil-layered water (twin bath)	500–5000
Cooling with liquid gallium	>5000
Cooling by conduction	>100000
Cooling by conduction mediated through a gas film	400–7700

For these plants, the practical upper limit of heat transfer coefficient  $h$  is around 300 W/m<sup>2</sup>K (Table 1). This condition limits the thermal tempering of soda–lime–silica glass to 3 mm and to 7 mm for borosilicate glass. Standard industrial thermal strengthening (current technology) of glass consists of a heating section where glass is heated to a predefined temperature in radiant or convection (or a combination of both heating techniques) heating furnaces then followed by a quenching section where glass is rapidly cooled by blowing ambient air to the glass surface. This cooling process is mainly convective where the heat transfer is performed by diffusion and advection through the air movement. The key point in the quenching phase is the temperature difference between the surface and the centre of the glass plate. On one side a larger temperature differential during the quenching phase may result in glass breakage (see Equation (6)). Once a cooling rate figure is fixed, breakage can be reduced starting the quenching phase at a higher temperature, though the higher temperature may result in excessive deformation of the glass plate during quenching. Thermal strengthening of thin glass requires higher cooling rate of glass surfaces resulting in a significant energy consumption. Air power consumption as a function of glass thickness increases exponentially<sup>(95)</sup> such that, to thermally strengthen a 2 mm glass, the required blower power can be estimated around 1200 kW/m<sup>2</sup>. This figure is technologically quite impractical for either plant and running costs. The present limit of blowing power industrially accepted is around 40 kW/m<sup>2</sup> which means a minimum soda–lime–silica glass thickness of 3 mm. With the aim to temper borosilicate or alkali borosilicate glass, different experimental arrangements have been proposed. The first idea<sup>(93)</sup> is the immersion of glass in oils.

The heat transfer coefficient is a function of the oil's viscosity. In particular, if viscosity decreases,

both heat transfer coefficient and oil inflammability rise. Adding volatile components like CCl<sub>4</sub> to oil significantly improves heat transfer coefficient. The other approach to improve heat transfer during the quenching phase is to use spraying systems with air/water mixtures.<sup>(93)</sup> The two vapour components of the quenching medium are carefully designed to keep a desired amount of air and amount of water ratio well controlled together with the mean droplet size of the water between 1 to 100 μm. Other elements to be considered in this approach<sup>(93)</sup> are the separation between glass surfaces and spraying nozzles (30–200 mm) and the spraying nozzle to adjacent spraying nozzle distance of between 30 to 60 mm. Probably the most popular method used is the so called twin bath tempering system where the quenching medium is a bath of water with a top layer of low viscosity oil (BP-GS 32).<sup>(92,93)</sup> To avoid the oil layer catching fire when the glass is immersed, a purging flow of nitrogen gas is used on top of the oil. There are still a number of drawbacks to this liquid/vapour contact strengthening, namely:

- (1) Thermal uniformity during the cooling phase leading to glass breakage
- (2) Complex handling of the plates or glass articles resulting in surface defects and temperature inhomogeneities leading to potential breakages.
- (3) Glass surfaces alterations due to the contact with liquids or vapours requiring post surface cleaning.

With the twin bath system it has been possible to thermally temper borosilicate plates with a thickness from 4 to 7 mm and borosilicate tubes,<sup>(92)</sup> 250 mm length, diameter 145 mm and wall thickness 6 mm, to a value of –95 MPa of surface compression. A 2 mm float glass (soda–lime–silica) has been successfully tempered with the twin bath technology to a surface compression up to –140 MPa.<sup>(92)</sup> The ceramic rolls conveying system, usually applied in most part of commercial plants, creates problems in the careful control of the symmetry of the quenching phase and in the quality of glass surfaces. New engineered solutions based on air supporting cushions have been proposed<sup>(96–98)</sup> allowing a better control of surface quality both in terms of waviness, anisotropy and defects and allowing the possibility to extend the lower thickness limit to soda–lime–silica glass to 2 mm. If the ceramic rollers contact is avoided, then the glass can be heated to a higher temperature before quenching. The air cushion support allows the technical possibility to achieve heat transfer coefficients with estimated values up to 400–500 W/m<sup>2</sup>K with a reduced blowing power of 400 kW/m<sup>2</sup> which reduces the blowing power needed to temper a 2 mm soda–lime–silica glass by a factor of 3. Even though this blowing power is an order of magnitude higher than conventional quenching power requested for conventional ceramic rolls conveying technology, it makes it pos-

sible to thermally strengthen 2 mm soda–lime glass. Recent studies<sup>(99)</sup> indicate the possibility to achieve a heat transfer coefficient of at least 5000 W/m<sup>2</sup>K using liquid gallium as the cooling quenching medium. The advantage of liquid gallium is in its lower vapour pressure, even at high temperatures, allowing preheating to a wide range of temperatures. By this technique, the thermal strengthening has been demonstrated of 3.3 mm, 1.75 mm and 1.1 mm of borosilicate glass with surface compressions, respectively, of 85, 60 and 20 MPa. There are still the above indicated drawbacks related to the quenching by a direct contact with a liquid. Solid contact thermal strengthening involving a direct contact of the hot glass surface with a cooler solid surface has been considered<sup>(100–102)</sup> based on the concept that heat transfer by conduction is far more effective than by convection. By solid contact the cooling is virtually instantaneous, only limited by the surface contact resistance due to the respective roughness of glass and heat sink surfaces. While this cooling method seems really effective, it brings serious drawbacks:

- Uneven contact over a large surface causing large thermal variations resulting in both potential breakages or huge birefringence variations.
- Surface defects due to glass/solid contact resulting in scratches, chips, and the like.

A recent breakthrough in the technology of thin glass thermal tempering and low thermal expansion thermal tempering has been proposed.<sup>(101,102)</sup> Elimination of the glass to solid contact drawbacks has been achieved by introducing the concept of conduction cooling mediated through a thin layer of a highly conductive helium gas. Helium has a thermal conductivity of  $\lambda_{\text{He}}=0.253$  W/mK versus  $\lambda_{\text{Air}}=0.047$  W/mK for air with gaps ranging from 31  $\mu\text{m}$  to 226  $\mu\text{m}$ . By this

Table 2. Results of thermal strengthening on different glass chemical compositions and thicknesses by using the conduction gas mediated quenching technique (after Lezzi et al<sup>(101,102)</sup>)

Glass type	Thickness $d$ (mm)	Helium gas gap ( $\mu\text{m}$ )	Temperature before quenching $T_A$ ( $^{\circ}\text{C}$ )	Surface compression $\sigma_c$ (MPa)
SLG	5.7	91	690	-312
SLG	3.2	84	690	-218
SLG	1.1	56	700	-176
SLG	1.1	65	700	-201
SLG	0.7	31	730	-206
SLG	0.55	25	720	-176
BS	3.3	119	800	Strengthening assessed by dicing pattern at fracture
SAS	1.5	226	790	Strengthening assessed by dicing pattern at fracture
SAS	1.1	91	800	-138
SAS	1.1	86	810	-201
SAS	0.1	141	820	Strengthening assessed by dicing pattern at fracture

SLG – Soda–lime–silica glass, BS – Borosilicate glass, SAS – Sodium aluminosilicate glass.

technology, full thermal strengthening for soda–lime, borosilicate and sodium aluminosilicate glasses with thicknesses down to 0.1 mm has been achieved. Table 2 shows results achieved using thermal quenching by conduction mediated with a gas film.

The results in Table 2 clearly represent a breakthrough in the possibility to thermally strengthen glasses with a wide chemical composition spectrum and with thicknesses down to 0.1 mm. It should be concluded that, as the glass thickness reduces to the ultra-thin glass limit<sup>(79)</sup> of 0.1 mm (100  $\mu\text{m}$ ), for sodium aluminosilicate glass, the strengthening by thermal means may become quite competitive relative to alternatives such as chemical strengthening (discussed below) in getting superior surface compression with comparable depths of compression layers at an acceptable process time.

### 3.4.2 Chemical strengthening of glass products

Chemical strengthening in glass has been reviewed extensively by Varshneya<sup>(1,103)</sup> and by Karlsson.<sup>(59)</sup> Chemical strengthening of glass products is based on the development of surface compression after alkali ions in the glass surface are exchanged one-to-one by larger sized alkali ions from a bath of molten salt at temperatures below the glass transition temperature. Thus, a sodium ion containing glass such as a soda lime silicate is immersed in a bath of  $\text{KNO}_3$  and a lithium aluminosilicate glass would be immersed in a bath of  $\text{NaNO}_3$ , all around 375–475 $^{\circ}\text{C}$ .

The physics of compressive stress development is similar to thermal stress development as in Equation (4) above (Cooper's analogy) and is explained in Ref. 104. The generated biplanar stress  $[\sigma_{yy}]_x$  or  $[\sigma_{zz}]_x$  at location  $x$  along the  $\pm x$ -direction of the diffusion is given by:

$$[\sigma_{yy}]_x = [\sigma_{zz}]_x = - \left[ \frac{BEC}{(1-\nu)} + \frac{BE}{2L(1-\nu)} \int_0^{2L} C dx \right] \quad (7)$$

$$\text{and } [\sigma_{yy}]_x = 0$$

One notes that, by analogy, the temperature  $T$  is replaced by molar concentration  $C$  of the invading alkali ion, and the linear thermal contraction coefficient  $\alpha$  is replaced by the "linear network dilation coefficient"  $B$

$$B = \frac{1}{3} \left( \frac{1}{V} \frac{\partial V}{\partial C} \right) = \frac{1}{3} \frac{\partial \ln V}{\partial C}$$

The volume network dilation coefficient is the expansion of molar volume when a unimolar exchange of alkali ions occurs and can be calculated by the molar volumes of compositionally equivalent as-melted ("CEAM") glasses.

Thus, for instance, a 15 $\text{Na}_2\text{O}$ –10 $\text{CaO}$ –75 $\text{SiO}_2$  (mol%) glass has a molar volume of 23.92  $\text{cm}^3$  at 723 K

(ion exchange temperature) which would expand to 26.4 cm<sup>3</sup> after exchanging all Na<sup>+</sup> ions with K<sup>+</sup> ions and allowing glasses to be in an after-melting condition. Complete suppression of this volume would yield 2.4 GPa compression. Varshneya *et al*<sup>(105)</sup> have clearly shown that, immediately after the ion exchange, fast relaxations (“β-relaxations”) set in which bring about rapid relaxation of the stress over nano- and microseconds. The volume following the β-relaxations is 25.24 cm<sup>3</sup>. Practically observed compression corresponds to the suppression of 1.32 cm<sup>3</sup> (=25.24–23.92 cm<sup>3</sup>).

Ion exchange is a diffusion behaviour; the kinetics of interdiffusion coefficient are controlled by an “interdiffusion coefficient”  $D$  such that

$$\bar{D} = \frac{D_{\text{Na}}D_{\text{K}}}{D_{\text{Na}}N_{\text{Na}} + D_{\text{K}}N_{\text{K}}} \quad (8)$$

The  $D_i$  are the self-diffusion coefficient of the alkali ions. The  $D$  is concentration-dependent, however, assuming it to be a constant, the penetration of the invading ions can be determined approximately at time  $t$  using the simple Gruzin solution<sup>(5,106)</sup> as:

$$C = C_0 \operatorname{erfc}\left(\frac{x}{2\sqrt{Dt}}\right) \quad (9)$$

Stress distribution and invading ion concentration as a function of depth can be plotted as that shown typically by Figure 5. They generally mimic each other, except that the interior must have area-balanced tension. The compressive stress profile and the tensile stress profile are separated by a neutral line, the depth below the surface is called the “DOL” (depth of layer); the compressive stress magnitude at the surface is called “CS” (compressive stress).

One may use typical values of the  $D$ s to suggest that the development of the DOL is quite slow. Using  $\bar{D} \approx 10^{-10}$  cm<sup>2</sup>/s, the chemical strengthening process would yield DOL=15 to 300 μm over several (4 to 24) hours of the strengthening experiment. This is unfortunate since, after several minutes of the diffusion process, viscous relaxation (“α-relaxation”) of the generated stresses also sets in. To provide adequate protection against handling flaws, one prefers to have deeper DOL over larger CS. Successful technology thus involves a careful optimization of time and temperature for the strengthening process. The overall stress development and its relaxation scheme is shown in Figure 5.<sup>(105)</sup>

In a commercial process, glass products are held in a stainless steel cage and lowered into an electrically heated steel tank. Glass containers may be placed loosely in steel cages making sure that they do not impact each other and lowered into the tank at an angle such that the container would fill. After the ion exchange treatment, the cage could be withdrawn, inverted to drain the salt and taken out of the tank. Flat glasses need to be introduced into the tank in a vertical orientation. They should be held in stain-

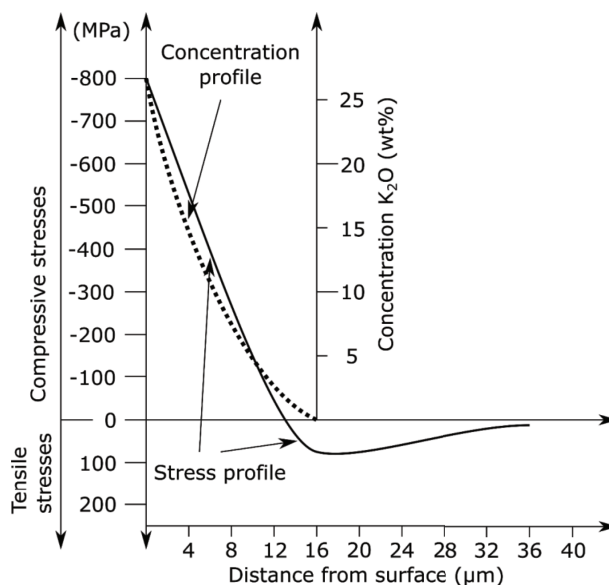


Figure 5. K<sub>2</sub>O concentration profile and stress profile as a function of depth followed by a ion exchange process, redrawn from Varshneya<sup>(107)</sup>

less steel clips with minimal and loose contact. Flat glasses which are thin (<1 mm) or super-thin (<0.4 mm) can warp during introduction into the tank due to temperature gradients.

Clay paste-based chemical strengthening is technologically easier to conduct. Glass containers are preheated at the opening of a tunnel, a paste containing clay–KNO<sub>3</sub>–water is either sprayed or coated uniformly or selectively.<sup>(108)</sup> The product travels through a gentle heat zone where the paste is dried. The coated product is exposed to ion exchange temperature and time, following which the product is cooled and washed to remove the adhering paste. Again, some caution needs to be applied to make sure that the product does not suffer from thermal shocking, with (heated) paste spray or coat. Unused salt may be recovered; the clay itself may be recycled. There are two primary impediments: the adherence of the paste layer to the glass surface after drying and the poisoning of the salt layer in immediate contact with the glass surface. Unlike a molten salt bath, the KNO<sub>3</sub> layer is relatively immobile, hence, the exiting Na<sup>+</sup> ions tend to poison the salt layer. For this reason, often the surface compression generated in paste-based strengthening is less than that generated using the molten salt immersion method.

At exchange temperatures of 375–475°C, soda–lime–silica (SLS) and sodium borosilicates (SBS) usually develop CS=–450 MPa with DOL=25 μm; a lithium aluminosilicate (LAS) generates CS=–350 MPa and DOL=250 μm, whereas a sodium aluminosilicates (SAS) on the other hand can generate as much as CS=–800 MPa and DOL=50 to 100 μm in a salt bath immersion process.

The technology effort would essentially be to freeze the strengthening process with as much suppressed

volume as possible. Even though common soda–lime–silica glasses are expected to develop higher initial surface compression than the sodium aluminosilicate glasses, the faster relaxation in SLS glasses results in surface compression which is significantly lower than in the SAS glasses. The compression profile in an SLS glass usually displays a maximum subsurface which tends to reduce the benefit. By the same token, it may be possible to develop much higher levels of surface compression by conducting an electric field-assisted ion exchange for short cyclic periods. Electrodes formed by salt-clay paste present a possibility for conducting electric field assisted chemical strengthening of flat and container glasses.

### 3.4.2.1 Technology issues

#### 3.4.2.1.1 Preheat and post-exchange heat

Glass products need to be lowered into a hot molten salt. Since the entire body cannot be submerged all at once, parts of glass are exposed to varying temperatures along its immersion dimension and wall thickness. This then creates transient thermal stresses which could fracture the product. High thermal expansion coefficient glass products often require a preheating schedule. This can be accomplished by placing a preheater on top of the molten salt tank. Glass should be preheated to within about 25°C of the salt temperature such that the eventual immersion will not generate substantial thermal stresses.

Post-exchange heating is yet another important step. Even though the glass has been strengthened, the process of retracting out of the molten salt bath can generate a large magnitude tensile stress on the surface which could overcome the compression and fracture the product. Thus, retraction should also be accomplished slowly. The issue here is the rapid relaxation of beneficial compression at elevated temperatures. A suggested procedure is to bring the temperature down rapidly in the “preheater”, and then withdraw the glass product slowly out of the preheater. Thermal treatments before chemical strengthening are relevant in those processes where glass articles are subjected to other technological processes at temperatures above glass transition. A typical example is the bending of flat glass to the requested shape, then chemically strengthened by ion exchange. The cooling down rate through the transformation temperatures range after bending may significantly alter the glass structure in a way that subsequent kinetics and stress build-up in the ion exchange process may lead to significant changes in surface compression and case depth. This topic has been reviewed by Zhang & Guo<sup>(109)</sup> who investigated the impact of preheating thermal history on physical properties and ion exchange attributes for glass formed by the fusion draw process. This preheating treatment has also been proposed for industrial applications by Allan *et al.*<sup>(110)</sup> Thermal treatments

after ion exchange have been recently studied from a theoretical approach by Macrelli *et al.*<sup>(111)</sup> where a new analytical solution has been proposed to a non-isothermal diffusion problem with variable boundary conditions. This analytical solution approach<sup>(111)</sup> can be used to predict residual stresses due to the incompatible strain from the molar volume mismatch between outgoing and incoming ions.

#### 3.4.2.1.2 Sensitivity to surface flaws, cage damage, post-handling abrasion

The usual DOL of 25 to 35 µm for SLS glass products makes the product sensitive to external abrasion by the cage steel and handling afterwards. The cage steel should be passivated often to keep its surface “shiny”. Staff should wear cotton gloves while handling the glass product. Use of robotics to handle the glass product to minimize handling damage is advisable. It is strongly advised that the product be transported over long distances (particularly when using common carrier) in paper “cell-packs”. Suitable protecting materials like steel or silica fibre fabrics are used to avoid a direct metal to glass contact.

#### 3.4.2.1.3 Dimensional changes

Ordinarily, for small glass products, one doesn't expect much of a volume swelling after ion exchange with larger ions. However, this is not true. As noted above, observed compression corresponds to a suppression of 1.32 cm<sup>3</sup>/mol of volume in a typical soda–lime–silica glass specimen whose original molar volume was 23.92 cm<sup>3</sup>/mol. The swelling corresponds to the magnitude of the interior tension. If we assume a large 0.5 mm thick plate with a 25 µm DOL on each side, equating the rectangular tensile area to triangular compression area, one estimates the tensile stress to be ~25/(2×250) of the compression. Thus, the fractional linear expansion would be roughly:

$$\frac{V_{m,CEAM} - V_m}{3V_m} \sigma_T \approx \left( \frac{1.32}{3 \times 23.24} \right) \left( \frac{25}{2 \times 250} \right) \approx 0.00095$$

Hence, for a 20 cm display plate, the increase in length is ~0.2 mm. In designing closely fitting spaces, one may need to make provision for the swelling.

#### 3.4.2.1.4 Warping of unannealed thin glasses

Even a mm thick glass plate may have unannealed residual stresses from prior processing. The problem of warping is particularly noticeable in float-produced thin glasses where the interdiffusion from the air surface has different kinetics than on the tinned surface. Cylindrical specimens in particular have residual surface stresses that are different in magnitude on the outside versus the inside. Often these stresses tend to relax at different rates during the ion exchange process. In turn, the differential relaxation is likely to cause warp. Such products should be pre-annealed carefully prior to subjecting them to the chemical

strengthening process. Methods have been developed to control warping, particularly for the float produced thin glasses.<sup>(112)</sup>

#### 3.4.2.1.5 Salt impurity buildup, degeneration and disposal

Technical grade  $\text{KNO}_3$  is usually 99% pure. Of the impurities, 0.1 to 0.25% is usually clay. With large tanks, the clay impurity itself builds up and, subsequently, deposits on the product which must be washed thoroughly. With continuing usage of the salt, the smaller sized ions (such as  $\text{Na}^+$ ) keep building up in the tank and begin to cause degeneration of the exchange potency. Concentration of  $\text{Na}^+$  in the salt bath is naturally increased by the ion exchange production operations. Excess of sodium ions in the bath reduces equilibrium potassium surface concentration in the glass, reducing, in turn, surface compression. In order to get a reasonable consistency of surface compression and case depth during the lifetime of the plant, excess potassium concentration is required to minimize effects of sodium. One may need to dispose of the salt (by pumping it out into steel barrels) and replenish the shortage periodically. Nitrate salts are oxidizers. Salt in the waste barrels is therefore classified "hazardous waste" and must be disposed to landfills in accordance with local laws. The disposal process can be a significant expense. In areas where agricultural land is predominant, it is possible to have farmers use adequately diluted waste salt as fertilizer for their land.

A reasonably ideal scenario is when the tank is treated with "getter" material to scoop out the waste ions and replace them with the invading ions. The search for a "proper" getter material requires extensive research, since it is sensitive to the actual salt composition. Some examples of getter material have been discussed by Xu *et al.*<sup>(113)</sup>

#### 3.4.2.1.6 Expense of electricity

The molten salt tanks should usually be kept at the operating temperature, unless a break in production is anticipated. In the latter case, tank temperatures should be lowered to around 250°C to make sure that the salt does not pick up atmospheric moisture and that the core of the electric heating elements also do not get penetrated by moisture. The constant consumption of electrical power represents a substantial operating cost. Computer-controlled power demand control is usually advisable.

### 3.4.3 Overglazing

Strengthening technology by overglazing a glass product is based on fusing a thin skin of a lower thermal expansion glass on both sides of a core substrate glass. The lower thermal expansion of the skin with respect to the core gives rise to a high compressive

stress in the skin and balancing tension in the core. An outstanding example of a commercial product which utilizes the 3-glass layers structure is Corelle® dinnerware. The product is made by pressing together a ~2 mm opal glass core between two thin layers (~0.15 mm) which act as the protective skin. The opal glass contains fluorine; hence, it is melted in a "cold crown vertical melter". Skin layers are separately melted and brought together around the core at the base of the core glass melter.

Dishes are shaped by pressing. Edges are rounded by a flame. In addition to the surface compression introduced by the differential thermal expansion, the ware is further tempered downstream using thermal tempering technology.

Overglazing by a lower thermal expansion glass can also be effected by a flame spray of a finely pulverized glass on the exterior surface of glass substrate selectively.<sup>(114)</sup> For instance, shoulders and the inside surface of a glass container do not require strengthening. This could be achieved during the transfer from parison stage over to the final stage in an IS machine. A "cased-gob" has also been attempted; however, the efforts did not enter the market place.<sup>(115)</sup>

Perhaps overglazing technology holds significant promise to strengthen glass products. In particular, it may be possible to introduce overglazing spray within the Individual Section ("IS") machine as an intermediate step between the parison making and the finishing stages.

#### 3.4.3.1 Wired glass and fire-resistant glass

Wired glass is made by incorporating a steel wire mesh at the midplane of a glass sheet. The rolled steel wire mesh is unrolled at synchronized speed with the semi-molten glass as it passes through a set of rollers to become a flat plate. The mesh sinks under gravity to reach the midplane. The mesh openings are usually squares or hexagons. Glass surfaces can be patterned. The primary purpose of the steel mesh is to retain glass in the case of breakage due to projectile impact, large vibrations, or fire. Wired glass is often used for doors, windows, ceilings and skylights.

There is another class of composite structure, mainly applied for fire-resistance, made of glass panes spaced with cavities (air gaps) filled with organic or inorganic gels. The purpose of this class of laminated glazing is to work as a fire-resistant transparent barrier providing structural integrity during a fire, and tightness against smoke and flames for a defined time (typically half an hour, one hour, or two hours) to allow evacuation of areas threatened by fire or eventually fire extinguishing. The main function is performed here by the material filling the gap between glass panes undergoing phase change either by intumescence or by ablation. The solutions adopted in commercial products are inorganic intumescent silicates (water glass)<sup>(116)</sup> or organic polyacrylamide composite.<sup>(117,118)</sup> Both

solutions are based on a phase change mechanism of heat absorption which blocks temperature rises during the fire providing effective thermal insulation to the not exposed glazing surface. The first is based on the intumescence properties of silicates while the second is based on the ablation mechanism of polymers.

### 3.4.4 Sustainability using lightweighted glass products

Lightweighted glass products have an immense potential to increase energy savings and reduce the environmental impact. There are several benefits with lightweighted glass products: raw material savings, energy savings, e-CO<sub>2</sub> reduction and transport savings. In response, glass bottles to contain pressurized beverages such as soda and beer have undergone a significant transformation. In the old traditional technology of the Individual Section (“IS”) machine, the container parison was made using an air-blow before transferring over to the finishing side for a second air-blow (“blow-and-blow”). The air blowing of the parison yielded significant variation in wall thickness around the hoop. To reduce the risk of a burst from internal pressure, wall thickness variation increased substantially (3–5 mm) such that the thinnest wall (around 3 mm) exceeded the minimum thickness requirement. This, in turn, caused the bottle to acquire considerable weight. Because of the high weight of glass containers, it has been difficult to justify recycling. The process of hauling the weighty glass container from the curbside over to some municipal collection point, sorting and transporting over to a glass melting site has simply been challenging in terms of the cost. Beginning with the 1970s, glass container producers watched their market share eroded by packaging alternatives such as plastics, paper and aluminium cans. In 1983, Emhart Corporation, the maker of the most popular IS machine, took a bold move in consultation with one of the authors (AKV), to seek approval from the US Dept of Justice to allow them to form an industry group of glass bottle makers to perform precompetitive R&D for the lightweighting of the glass container. This group, called the “International Partners in Glass Research” initiated several projects around the globe with the aim of reducing the bottle weight by ~30%. Some of the technologies nucleated several ideas for lightweighting. Others were developed independently. Some of the more promising ones are listed below:

- (1) IS machine with press-and-blow
- (2) Overglazing
- (3) Thermal tempering
- (4) Chemical strengthening using molten KNO<sub>3</sub> salt immersion
- (5) Chemical strengthening by clay-paste-based KNO<sub>3</sub> strengthening

By far, the most successful technology is the IS

machine fitted with press-and-blow scheme. The variation in wall thickness due to air-blow has been significantly reduced by using a plunger press to form the parison before transfer over to finish by an air-blow. Wall weights have indeed been reduced in many cases by as much as 25%.<sup>(115)</sup>

The overglazing by a flame spray of reduced thermal expansion layer can be incorporated in an IS machine. We conclude that an IS press-and-blow machine fitted with an overglazing step for glass strengthening holds considerable promise for next generation lightweighted glass products. A next option perhaps is post-forming strengthening by thermal or chemical means, which will be investigated for sustainability in a forthcoming paper.<sup>(119)</sup>

As discussed above, thermal tempering technology for thin-walled glass has now progressed enough to be a serious contender for our lightweighting efforts. Diffusion based technologies, namely chemical strengthening whether immersion-based or clay-paste-based, perhaps will not gather much momentum due to the time required for the generation of a meaningful DOL unless some disruptive technology is developed to take advantage of electric field assistance. The latter has, however, been much less studied than thermal tempering and requires further research and development as well as a process invention to be effective.

### 3.5 Management of glass composition to optimize the strength: search for the ideal “Gorilla”

Gorilla® and Dragontrail® glasses are the most modern developments in the use of thin strengthened glasses for displays in personal mobile communication electronics such as mobile phones, MP3 players, and automobile windows, in an effort to reduce the vehicle weight. Pioneering work in this field was conducted by Varshneya.<sup>(120)</sup> However, it is an area where much work is still needed. Because of the belief that glass strength was essentially controlled by the severity of surface flaws, and not by chemical composition, not much research was conducted on the effect of glass composition on the strength and fracture behaviour. The most significant research in this direction was reported by Sehgal & Ito,<sup>(121,122)</sup> who showed that the indentation “brittleness” of a glass varied with density, showing a pronounced minimum at some value. The location coincided with the crossover from a “normal” behaviour (development of a pileup around the indent) to an anomalous behaviour where no pileup was observable. The glass composition corresponding to this value was called “low brittleness” glass. In reality, density was not the cause of low brittleness. It itself was an effect of the specific composition. It is now understood that intrinsic flaw formation and extrinsic flaw propaga-

tion are all dependent upon the network hydrostatic and deviatoric yield strengths. Thus, it is natural to expect that the glass composition will have a significant influence on the strength of glass.

The physical properties  $E$  and  $\gamma_s$ , thought assumed constant, do vary. At high applied stress levels, glass is apt to show nonlinear elasticity, which implies that  $E$  itself depends upon the magnitude of the strain. Likewise, the fracture surface energy must be understood to be different from the usual surface energy (often quoted at 0.35 J/m<sup>2</sup>). While the latter is the potential energy of a free surface with atomic locations disturbed due to an imbalance of network potentials in equilibrium irrespective of the environment, the former involves nonlinear stretching of atomic bonds gradually over several atomic layers with storage of nonlinear elastic energy. Whereas physical properties such as the Young's modulus and the fracture surface energy do determine the strength as per Equation (1), the effect of glass composition on the yield strengths which control the stress field around a flaw is paramount. The yield strengths, in turn, are influenced by the network connectivity. The subject is termed "topological engineering". It is incorrect to think that infinite yield strengths leading to perfectly elastic deformations during indenting is the ideal scenario for maximized glass product strength. In such a situation, stress fields continue to build until failure occurs. The ideal condition is when the shear yield strength is high, and the hydrostatic compressive yield strength is low. In networks that are optimally connected (degrees of constraints at connections equal degrees of freedom), the shear yield strength is maximized, as argued for a non-oxide glass.<sup>(123)</sup> The lack of pileup around the indent in the low brittleness glass is indicative of a high shear yield strength. Open structure networks encourage low compressive yield strength.

As discussed by Mauro *et al*,<sup>(124)</sup> the damage resistance of glass can be significantly improved by incorporation of trigonally coordinated boron into the glass network. Boron can exist in either threefold or fourfold coordination states in the glass. Threefold coordinated boron offers a more open structure and the ability to compact under a mechanical load, e.g. as occurs during indentation or scratching events. Whereas normal glasses crack in a brittle fashion after exceeding their elastic limit, glasses with threefold-coordinated boron can yield plastically in response to a mechanical load, causing the glass network to densify and prevent buildup of stress field. This then enhances the indentation crack threshold by a factor of three or more. A similar advantage can be gained by suppressing lateral crack formation during a scratch event. The behaviour, termed intrinsic damage resistance, is a highly effective way to suppress crack formation in everyday glass products.

One would anticipate that, in the near future, suit-

able glass compositions will be developed which have an optimized network connectivity that would enable these glasses to be made into extremely thin-walled lightweight glass products where not only will the intrinsic flaw generation be minimized but also the hardness will be greatly increased, making it difficult for indents to cause cracking; the crack propagation velocity will itself be reduced. Such glasses will additionally be capable of being strengthened more quickly and more easily.

### 3.6 Management of energy absorption (glass lamination)

We refer here to a glazing made of multiple plies of glass panes kept together by interlayers. By definition we are considering a composite structure made of different materials with different mechanical, thermal and chemical properties. Laminated glazing is a composite material combining inorganic glass properties with the characteristics of tough yet elastic polymeric (organic) interlayers. The lamination processes is performed at temperatures far below glass transition temperatures where interlayer materials are usually polymers with a viscoelastic mechanical behaviour. In 1909 the French chemist Eduard Benedictus invented and patented<sup>(48)</sup> the laminated glazing with a polymer and named it TriPlex<sup>®</sup>. As in many important inventions it is reported that the finding was by chance after an unwanted event where a supposedly empty glass flask was accidentally broken, but contained a polymer (cellulose nitrate) in a solvent that after solvent evaporation left a thin plastic film that was able to keep the glass fragment together. The industrial applications followed rapidly but were not always blessed by fortune: discolouring, glass shard penetration of polymers and eventually delamination were the main issues to be faced. In 1927 the Canadian chemists H. W. Matheson & F. W. Skirrow invented<sup>(125)</sup> the plastic polyvinyl butyral (PVB) and the first structured patent of safety glass made with this interlayer was filed by Fix.<sup>(126)</sup> Since that time laminated glass with plastic interlayer became an increasing standard for windscreens in the automotive industry and, presently, it is recognized by authorities (ECE in Europe and ANSI in US) as a standard product subject to homologation rules. Laminated glass products generally have strengths which are barely higher than the unlaminated product; the main advantage of laminated glass lies in the post-breakage behaviour of the composite structure in retaining the potentially dangerous glass splinters and shards and providing safety. In Table 3, the definition of three "classes of consequences" are defined in terms of adverse events after the failure of a glass component.

The classification of laminated glass, defined as above, depends primarily on the characteristics of

Table 3. Definition of the Consequences Class concept (from the European Standard Draft TS 19100)

Consequences class	Description	Examples of buildings and civil engineering works
CC3	<b>High</b> consequence for loss of human life, or economic, social or environmental consequences <b>very large</b> .	Grandstands, public buildings where consequences of failure are high (e.g. a concert hall).
CC2	<b>Medium</b> consequence for loss of human life, or economic, social or environmental consequences <b>considerable</b> .	Residential and office buildings, public buildings where consequences of failure are medium (e.g. an office building).
CC1	<b>Low</b> consequence for loss of human life, or economic, social or environmental consequences <b>small or negligible</b> .	Agricultural buildings where people do not normally enter (e.g. storage buildings and greenhouses).

the laminating interlayer. We can identify interlayers made of viscoelastic polymeric films ranging typically from 0.3 to 1.25 mm (as a single film) that can be easily layered to reach total interlayer thicknesses of several millimetres, and interlayers made of cast polymers (mainly acrylics) that are then cured mainly by UV radiation. The first type of interlayers can be further segmented into the following class of polymers (Table 4).

PVB is likely the most widely used interlayer material; it requires a laminating cycle at temperatures ranging from 120 to 140°C combined with autoclaving at pressures from 0.9–1.3 MPa and a de-airing system (to eventually evacuate air trapped in the interfaces) that could be a vacuum bag or nipple rollers. A key issue, often not discussed in detail, is the role played by the adhesive bond of the interlayer with glass plies. Both high and low levels of adhesion may be intentionally designed according to the final purpose of the laminated construction. A high

level of adhesion is beneficial to guarantee that, in case of glass breakage, potentially dangerous glass fragments are not released but stay firmly attached to the interlayer. High levels of adhesion are also beneficial for static or quasi static loads, as the whole laminate behaves as a solid structure with a full mechanical collaboration between the glass plies. The level of mechanical collaboration between the glass plies is dominated also by the shear modulus of the interlayer. Figure 6 reports values for different types of polymers and their dependence on load duration and temperature. From another perspective, a low level of adhesion provides better performances in impacts, allowing the absorption of a considerable amount of impact energy by detaching from the glass and allowing a better elastic deformation of the interlayer. The level of adhesion of interlayers with glass surface is dominated by the surface chemistry of glass with mainly silanol groups Si–OH formed on the glass surface by water absorption. Some polar

Table 4. Class of transparent polymers used for glass lamination

Type of polymeric interlayer	Short identification	Chemical formula/structure
Polyvinyl butyral	PVB	
Ethylene vinyl acetate	EVA	
Thermoplastic aliphatic polyurethane	TPU	<p>U = diisocyanate      ——— hard segment       = polyol G = chain extender      ~~~~~ soft segment</p>
Ionomeric resin	SGP	

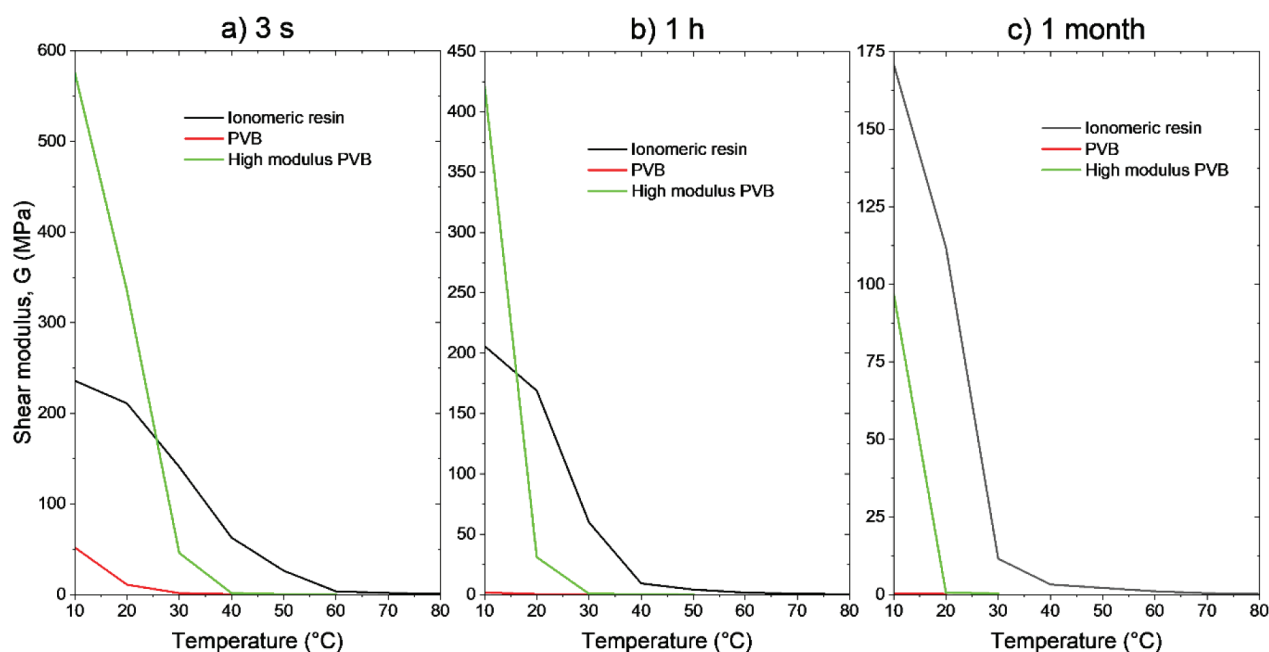


Figure 6. Shear modulus of ionomeric resin and PVB interlayers as a function of temperature for (a) short term load (3 s), (b) mid term load (1 h) and (c) long term load (1 month) [Colour available online]

components of the interlayer (polyalcohol groups in PVB) or the use of adhesion promoters such as silanes, matching the surface chemistry of glass and the one of interlayers, allows the formation of a dense network of hydrogen bonds or eventually true chemical bonds.

Laminated glazing is presently used in automotive glazing where all windscreens are made of such type of construction with glass layers ranging from 1.6 to 2.1 mm with a PVB foil of 0.38 or 0.76 mm. The interlayer is modified by introducing infrared absorbing nanoparticles to provide solar protection functionality or layered with different mechanical characteristic to provide damping of vibrations to improve acoustic performances. An obvious application of laminated glazing is in building and architectural environments to provide both safety and security features. Remarkable applications are in marine environments where complex laminated constructions made of multiple glass plies can withstand hydrostatic pressures up to several bars (100 to 300 kPa).

In the present discussion, we have considered static or quasi-static loads configurations (wind load, hydrostatic load, human load as either point loads or linear loads) or the capability of laminated glazing constructions to provide protection against impacts, either accidental or intentional.

Another remarkable application lies in the capability of laminated constructions to withstand high rate impact situations like bullets with speeds up to 1000 m/s, or massive missiles from hundreds of grams to several kilograms (EN 15152) travelling at speeds from a few tens of metres per second to hundreds of metres per second, including high speed windscreens for trains or aircraft (ASTM F

330) subject to the so called bird-strike test. In these high-rate load scenarios, temperature is relevant. At low temperatures (around  $0^{\circ}\text{C}$  or below) some interlayers (like PVB) become fragile and do not really provide the desired level of mechanical performance. In these last situations, TPU interlayers are preferred due to their capability to maintain the desired viscoelastic characteristics even at a few tens of degrees Celsius below zero. Shear modulus of three example interlayers (ionomeric resin, PVB and high modulus PVB) as a function of temperature and time is shown in Figure 6. Laminated constructions where glass plies are coupled with the innermost layer (opposite to the point of impact) of polycarbonate or polyethylene terephthalate (PET) have anti-spall characteristics. These are mainly used in armoured glazing with antibullet performances. For lamination of glass with polycarbonates, the interlayer cannot be PVB because of the lack of capability to match the relative deformations of glass and polycarbonate resulting from the mismatch of the thermal expansion coefficients. In such assemblies, the preferred interlayer is again TPU. The mechanical behaviour of a laminated glazing with  $n$  glass plies of individual thicknesses  $t_j$  ( $j=1, n$ ) depends on the level of collaboration of the plies that, in turn, depends on the shear modulus and thickness of the interlayers. In the case of perfect stress transfer from the loaded ply to the others, the structure behaves as a monolithic glass with a thickness given by  $t_t$  which is the sum of the  $n$  glass plies and of the  $(n-1)$  interlayers. In the case of no collaboration, corresponding to a shear modulus of interlayers  $G=0$ , it can be demonstrated that the structure behaves with an equivalent thickness for

each ply  $t_{eqj}$ :

$$t_{eqj} = \sqrt{\frac{\sum_{i=1}^n t_i^3}{t_j}}; j = l, n \tag{10}$$

In the case where the glass laminate is made of all plies with the same thickness  $t_j=t$  then the equivalent thickness is:

$$t_{eq} = \sqrt{\sum_{j=1}^n t_j^2} = t\sqrt{n} \tag{11}$$

In the case of different thicknesses, a natural choice of an “equivalent thickness” for structural calculations is:

$$t_{eq} = \min[t_{eqj}]; j=l, n \tag{12}$$

Several approaches have been presented in the literature<sup>(127–135)</sup> for the evaluation of an “equivalent” or an “effective” thickness of a laminated glazing for intermediate mechanical collaboration situations and for dynamic load rate.<sup>(136)</sup> In case of complex or controversial situation, a numerical approach based on finite element analysis is recommended. To correctly model high loading rate phenomena (bullet or missile impacts), proper material mechanical characteristics need to be determined from characterization methods at a comparable loading rate.

### 3.7 Strength testing in commercial environments

Strength testing of glass is rather complex when going into details of the factors influencing the test, e.g. loading type, loading rate, sample preparation procedure, surface condition of the sample, tempera-

ture, and humidity. Test results depend greatly on the size and distribution of the inevitable flaws or defects in the surface.

#### 3.7.1 (Instron) 4-pt beam, ring-on-ring

There are several standardized tests for flat glass, e.g. four-point bending test, three-point bending test, and ring-on-ring test, see Figure 7. All these tests can be conducted using a uniaxial testing machine, frequently called a universal testing machine, equipped with the proper fixtures for the test.

The four-point bending test is standardized for glass in buildings through ISO 1288-3 but also through, e.g. ISO 14704, ASTM C1161 and IEC 61747-40-2. The test method and fixture are shown in Figure 7(a); the flexural stress is given by

$$\sigma_f = k \left[ F_{\max} \frac{3(L_s - L_b)}{4Wd^2} + \sigma_{bg} \right] \tag{13}$$

Where  $\sigma_f$  is the stress at midpoint.  $F_{\max}$  is the maximum load, i.e. the load at breakage,  $L_s$  and  $L_b$  are the distances as given in Figure 7(a),  $W$  is the specimen width,  $d$  the specimen thickness and  $k$  a dimensionless factor that depends on the central deflection and  $d$  as described in ISO EN 1288-3. In the ordinary case,  $k$  is equal to 1.  $\sigma_{bg}$  is the bending stress imposed by the self-weight of the specimen and is given by

$$\sigma_{bg} = \frac{3\rho g L_s^2}{4d} \tag{14}$$

where  $\rho$  is the density of the specimen and  $g$  the gravitational acceleration.

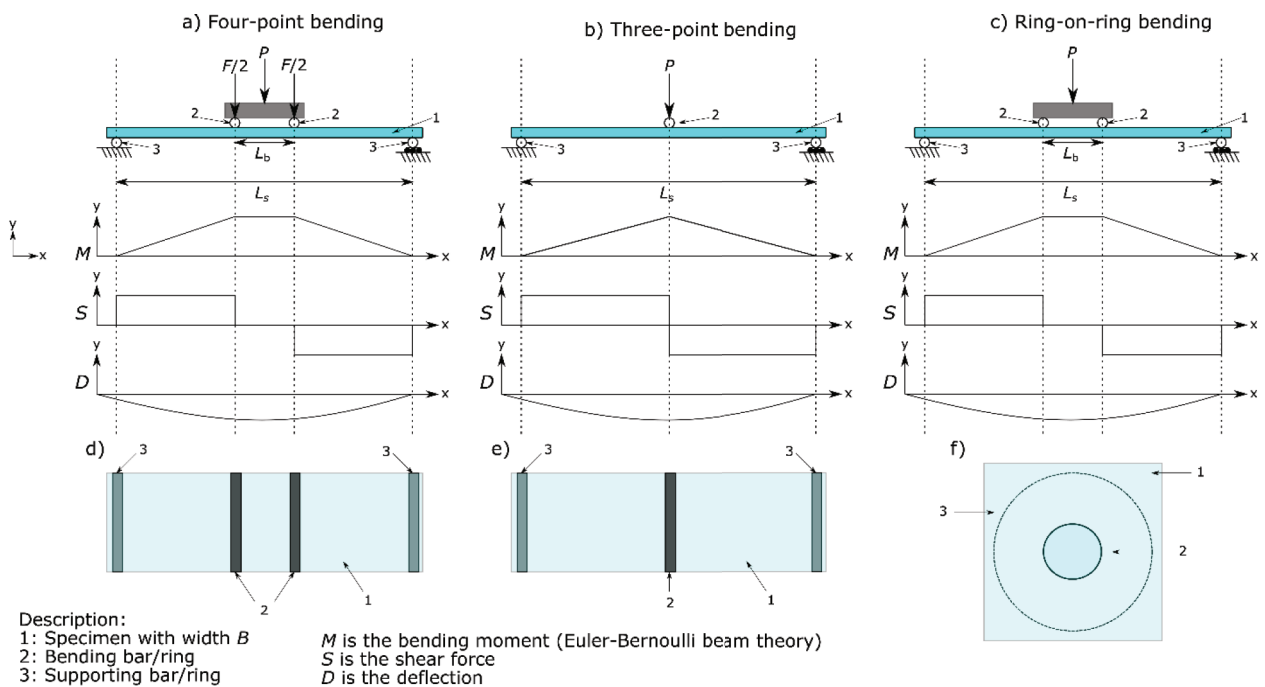


Figure 7. Schematic principles of four-point bending, three-point bending and ring-on-ring bending including schematic graphs of the bending moment ( $M$ ), shear force ( $S$ ) and deflection ( $D$ ) [Colour available online]

The three-point bending test is not as standardized as four-point bending but there are standards, e.g. EN 2746, and it is still used in industry or by individuals not as well experienced in structural mechanics. However, it is also used for fracture toughness testing using the single notched beam methodology. The principles are very similar to four-point bending as can be seen in Figure 7(b).  $\sigma_f$  is given by

$$\sigma_f = k \left[ F_{\max} \frac{3L}{2Wd^2} + \sigma_{bg} \right] \tag{15}$$

for a rectangular cross section.

The ring-on-ring test is standardized and described in ISO EN 1288-2 and 1288-5 as well as ASTM C199-19. The principle is shown in Figure 7(c) where a glass specimen is placed inbetween a loading and a supporting steel ring. The ring-on-ring test<sup>(137,138)</sup> has two features that makes it interesting to use: (i) it creates a homogeneous biaxial stress field inside the loading ring and (ii) the edges of the specimen are not stressed as much. The equibiaxial failure stress ( $\sigma_t$  and  $\sigma_r$  being the tangential and radial stresses) can be calculated based on a solution from the Kirchoff–Love theory according to

$$\sigma_t = \sigma_r = K \frac{F_{\max}}{d^2} \tag{16}$$

where  $K$  is a correlation coefficient given by

$$K = \frac{3}{\pi} \left( (1-\nu) \frac{1-(r_1/r_2)^2}{(r_3/r_2)^2} - 2(1+\nu) \ln \frac{r_1}{r_2} \right) \tag{17}$$

Where  $r_1$ ,  $r_2$  and  $r_3$  are the radii of the load ring, support ring and the glass plate, respectively. However, square specimens are frequently used and therefore  $r_3$  can be defined as the characteristic length of the samples,

$$r_3 = \frac{\sqrt{2}+1}{4} W$$

### 3.7.2 Pendulum swing

The pendulum hammer impact swing test is standardized through EN 12980 and is suitable for prod-

ucts such as glass bottles, jars, drinking ware glasses, vases, etc. The schematics are shown in Figure 8; the method uses a pendulum hammer with weight  $m$  raised to an angle  $\varphi$  to impact a glass article by free fall. Based on  $m$ , the pendulum length  $L_p$  and height of pendulum  $h_p$ , a relationship to calculate the impact energy ( $U_{tot}$ ) is given by the sum of the kinetic ( $U_K$ ) and potential energy ( $U_p$ ),

$$U_{tot} = U_K + U_p = \frac{m(\sqrt{2gh_p})^2}{2} + mgh_p \tag{18}$$

where  $h_p$  relates to the angle  $\varphi$  by  $h_p=L_p(1-\cos\phi)$ .  $L_p$  is usually in the range 0.2–0.7 m and the hammer weight is 0.1–1.0 kg. The test procedure is to progressively increase the angle  $\varphi$  until the glass product chips, cracks or fractures; alternatively, until a predetermined impact energy level is reached.

For architectural glass, there is a larger pendulum impact test, EN 12600; the principles are the same but, in the test, a softer material, such as a pneumatic tyre, should be used as the impact giving pendulum.

### 3.7.3 Ball drop

The ball drop test is a common standardized test for flat glass; it is, for instance, used for laminated flat glass (ISO 16936-1, ASTM F3006-20 and ASTM F3007-19) and for handheld electronic device cover glass (IEC 61747-40-3 and IEC 61988-4-2). The test is carried out using a setup shown in Figure 9. The ball is a steel ball that is released using a mechanism that does not interfere with the free-fall energy given by the gravitational acceleration, e.g. electromagnetic or vacuum assisted. The specimen holder can be square or rectangular and is made of a rigid polymer to minimize damage to mounted glass specimens. It should also be large enough so that no glass specimen touches the base by deflection during a test. The ball drop test is a repetitive test which means that one starts with a low height and then increases the height of the ball until the glass specimen breaks, allowing only one hit of the ball on the specimen on each height. The height differences are typically 5 cm and ball should hit the centre of the glass specimen.

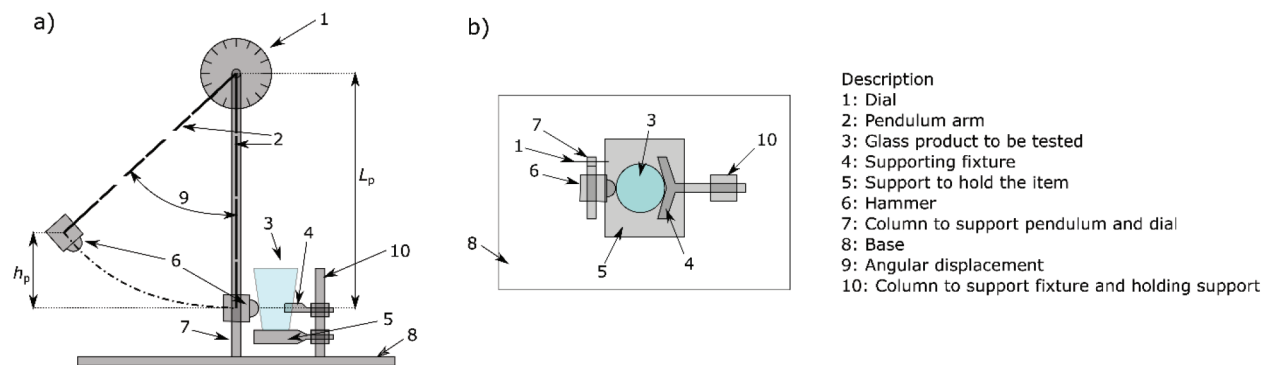


Figure 8. Schematics of a pendulum impact testing equipment [Colour available online]

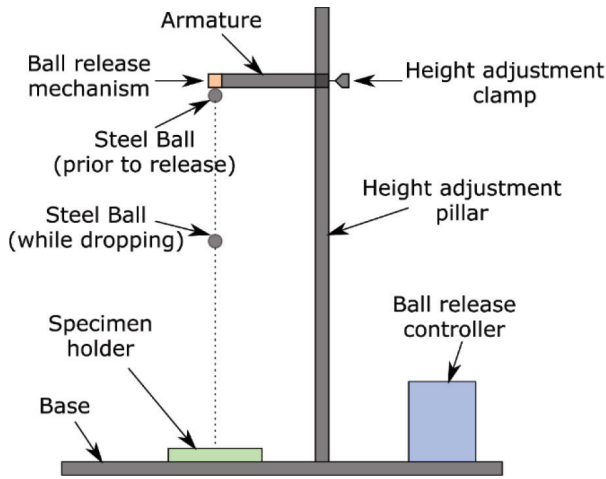


Figure 9. Schematics of a ball drop test setup [Colour available online]

The fracture energy  $U_b$  in J is calculated by

$$U_b = \frac{m}{1000} g \frac{(h+c)}{100} \quad (19)$$

where  $m$  is the mass of the ball in grams,  $g$  the gravitational acceleration,  $h$  the height of the armature, and  $c$  a correction factor for specimen’s nominal thickness variation.

### 3.7.4 “Chicken cannon”

The “chicken cannon”, sometimes referred to as the “chicken gun”, is a bird flight impact simulator test using compressed air to bombard bird carcasses onto aircraft components. The purpose is to simulate high speed bird strike impacts during flight; windshields are among the most vulnerable, and therefore most tested, products. The equipment has earned the name “chicken gun” as (thawed) chickens nominally 1.81 kg in weight were the most commonly used ammunition. However, nowadays, a chicken dummy such as a 1.81 kg gel has also been developed.<sup>(139)</sup> The speeds involved during an aircraft and bird collision can be considerable, often ca. 350 km/h, resulting in a massive transfer of kinetic energy. The earliest test of windshields is reported in 1943.<sup>(140)</sup> It showed

that glass panels were easily penetrated by a 1.81 kg bird at only 121 km/h; however, with a polyvinyl chloride lamination, the windshield glazing could be made more resistant. The test is standardized by ASTM F330-21 and aircraft windshields need to be certified for use in aircrafts. Nowadays, in addition to experimental testing, (see Figure 10 for a representative air gun), finite element methodology can be used to assess the safety.<sup>(141)</sup> Also other vehicles, such as trains and cars, particularly high speed vehicles, need to be designed for impact with a bird.<sup>(142)</sup>

### 3.7.5 Burst pressure

When glass bottles are used for carbonated liquids, e.g. soft drinks, beer, sparkling wine, they are exposed to internal hydrostatic pressure.<sup>(143)</sup> Therefore, a burst pressure test has been developed and standardized through ISO 7458 and ASTM C147. The ISO 7458 standard is separated into two different methods both of which use tap water as the medium. Common to both methods is that there needs to be a resilient seal to keep the pressurizing medium constant during the test. The temperature of the glass container and the water should not differ by more than  $\pm 5^\circ\text{C}$ . An example of the effect of hot- and cold-end coated glass containers on the burst pressure has been studied by Bhargava *et al.*<sup>(144)</sup>

Method A involves application of a uniform internal hydrostatic pressure for  $60 \pm 2$  s. Another predetermined period of time may also be used but then the pressure values must be corrected to those which would be obtained for a 60 s test. The uniform internal hydrostatic pressure can be progressively increased in increments of 1 or  $2 \pm 0.1$  bar (0.1 or 0.2 MPa) until 50 or 100% of the glass containers have been broken.

Method B involves increasing the internal hydrostatic pressure at a constant (but to within a  $\pm 2\%$  reproducible) rate of  $5.8 \pm 1$  bar/s ( $0.58 \pm 0.1$  MPa/s) until the container fails or a predetermined level is reached.

An empirical relationship between the ramp pressure test (method B) and 60 s pressure test (method

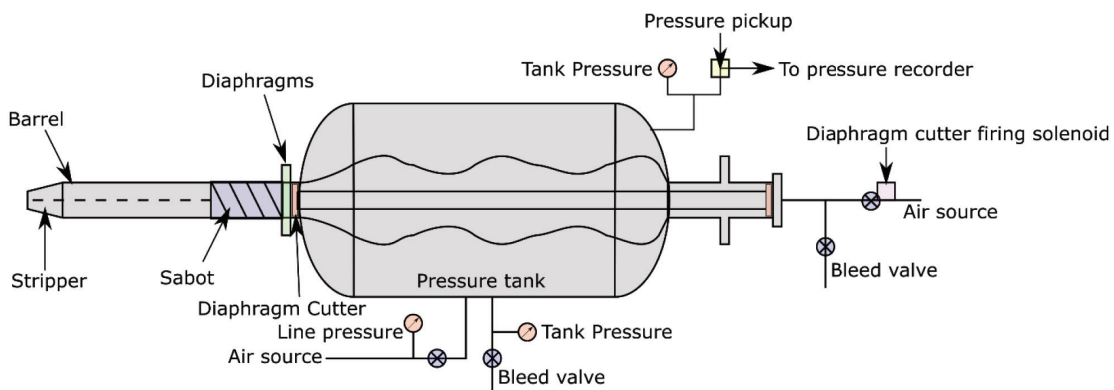


Figure 10. Representative sketch of Air Gun, redrawn from ASTM F330-21 [Colour available online]

Table 5. Applicable missiles for the ASTM E1996 test

Missile level	Missile test	Missile mass specification	Missile dimension specification (w×h×l)	Impact speed
A	Small	2 g±5% steel balls	N/A	39.62 m/s
B	Large	910 g±100 g	50.8×101.6×525±100 mm	15.25 m/s
C	Large	2050 g±100 g	50.8×101.6×1200±100 mm	12.19 m/s
D	Large	4100 g±100 g	50.8×101.6×2400±100 mm	15.25 m/s
E	Large	4100 g±100 g	50.8×101.6×2400±100 mm	24.38 m/s

A) is given by

$$P_R = 1.38P_{60} + K \tag{20}$$

where  $P_R$  is the actual pressure,  $P_{60}$  the 60 s pressure and  $K$  a constant equal to 1.783 bar (0.1783 MPa).

### 3.7.6 Small and large missiles for hurricane code

Windborne debris may cause a lot of damage and possible injuries, if materials such as window glazing do not withstand their impact. Hurricanes are classified according to the Saffir–Simpson scale, C1: 33–42 m/s, C2: 42–49 m/s, C3: 49–58 m/s, C4: 58–69 m/s and C5: >69 m/s, typically used in North America, so it is worth noting that other scales are used in Europe (Beaufort scale) and there are other scales for tornados, e.g. Fujita’s scale and TORRO scale. In order to cope with wind debris impacts, small and large missile tests have been designed and are standardised according to ASTM E1996 and TAS 201. The ASTM E1996 missile test involves small and large missile tests according to the specifications in Table 5. Depending on the wind zone, Table 5 specifies the level of protection required (unprotected, basic or enhanced protection) and which test needs to be fulfilled. The pass/failure criteria is relatively complex and therefore not repeated here.

### 3.7.7 Hopkinson bar

The Hopkinson bar, sometimes also called the split-Hopkinson pressure bar (SHPB), is an apparatus and

test of the dynamic stress–strain response of materials at high strain rates, typically in the range of 50 to 12000 s<sup>-1</sup>. It is named after Bertram Hopkinson who first suggested it as a way to measure stress pulse propagation in a metal bar.<sup>(145)</sup> The method has then been further developed by Kolsky,<sup>(146)</sup> therefore the test is sometimes also called the Kolsky bar to incorporate advancements in the cathode ray oscilloscope that Davies enabled.<sup>(147)</sup> The method has since been modified to allow for tensile, compression and torsion testing as well. The design of the sample and apparatus can be varied to adapt to different types of tests but the principle is the same and is shown in Figure 11.<sup>(148)</sup> As the striker bar hits the incident bar, a stress wave propagates through the material toward the glass sample, that absorbs, reflects and transmits parts of it. Assuming that the deformation in the glass sample is uniform, the stress and strain can be calculated from the amplitudes of the incident, transmitted, and reflected stress waves. For 1-D linear elastic waves,<sup>(148)</sup> the forces ( $P_1$  and  $P_2$ ) acting on the two ends of the specimen can be calculated by

$$P_1 = A_i E_i (\epsilon_i + \epsilon_r) \tag{21}$$

$$P_2 = A_t E_t (\epsilon_t) \tag{22}$$

where  $A_1$  and  $A_2$  are the cross-sectional areas of interface  $X_1$  and  $X_2$ ,  $E_i$  and  $E_t$  are the elastic moduli of the materials for the incident and the transmission bar and  $\epsilon_i$ ,  $\epsilon_r$  and  $\epsilon_t$  are the recorded strains of the incident, reflected and transmitted wave. Assuming that the materials of the incident and transmission bar are the same, the strain rate  $\dot{\epsilon}_{ic}$  and strain  $\epsilon_{ic}$  of

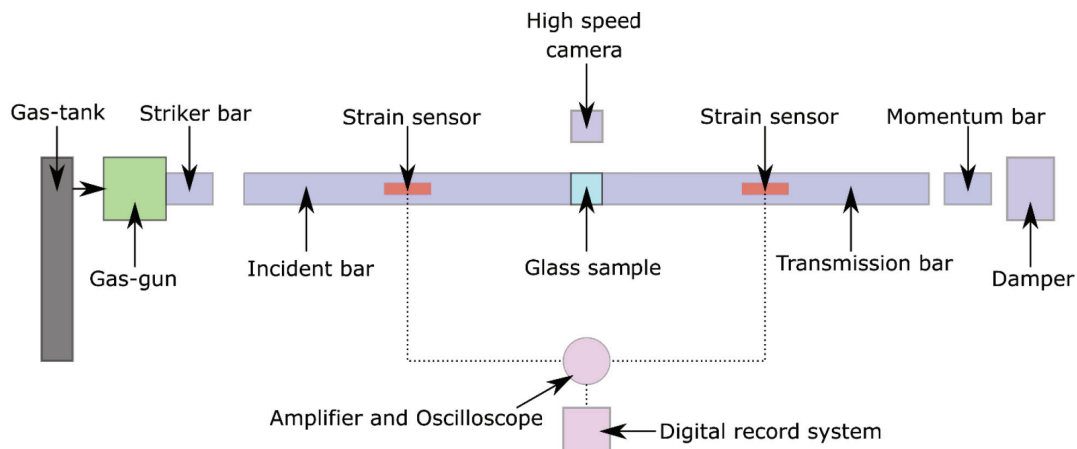


Figure 11. A schematic of the principal setup of the split-Hopkinson pressure bar (SHPB) test for compression. The stress sensors are typically strain gauges but may also be fibre Bragg grating (FBG) sensors<sup>(149)</sup> [Colour available online]

the glass specimen can be calculated from

$$\dot{\epsilon}_{ic} = -\frac{2c_0}{L_s} \epsilon_r \quad (23)$$

$$\epsilon_{ic} = -\frac{2c_0}{L_s} \int_0^t \epsilon_r dt \quad (24)$$

where  $L_s$  is the specimen length and  $c_0$  the elastic wave speed in the bars that can be calculated from the elastic modulus and the density of the material,  $c_0 = \sqrt{E/\rho}$ .

### 3.7.8 Edge-on impact test

The edge-on impact test is a test to study the crack and fracture propagation upon impact from a high speed projectile.<sup>(150,151)</sup> The schematic setup is given in Figure 12. At high stress rates, the surface defects that otherwise usually determine the strength of glass become less of a controlling factor. Instead, nucleation of bulk/volume defects play an important role. The glass fracture can be studied using a high speed camera with or without polarizing and retardation filters to view, e.g. strains in colour. Using image analysis it is then possible to determine the fracture (or damage) propagation speed.<sup>(152)</sup> The damage, the strain- or stress-rate and their effects on the strength have been the subject of development of models.<sup>(150,152)</sup> It is still a developing topic to understand what happens to glass under high strain-rates.

### 3.7.9 Statistics of glass strength tests

Evaluation of strength tests of glass most often involves using statistics to cope with the unpredictable and distributed strengths of glass. To obtain enough data, it is advised to test at least 10–20 specimens depending on which state of reliability that is wanted. The strength data ( $\sigma_i$ ) should then be ordered based on their fracture probability ( $F_i$ ) that can be calculated by

$$\{\sigma_i, F_i\} = \sigma_i, \frac{i}{N} \quad (25)$$

where  $i$  denotes the sample  $i$  and  $N$  the size of the sample population. The fracture probability can then be fitted to a statistical distribution. The Weibull distribution, due to its weakest-link theory, has found widest acceptance and use for glass, although a normal (Gaussian) distribution is also used.<sup>(153)</sup> The Weibull cumulative distribution function is given by

$$F(\sigma) = 1 - e^{-\left(\frac{\sigma_i}{\sigma_c}\right)^m} \quad (26)$$

where  $\sigma_c$  is the characteristic strength and  $m$  the Weibull modulus. These can then be transformed into straight lines by plotting  $\{-\ln[\ln(1-F(\sigma))]\}$  versus  $\{\ln(\sigma_i)\}$ . If there are different fracture modes, a 3-parameter Weibull distribution may have to be used. By taking time and stress corrosion into consideration, it is possible to make lifetime predictions of glass products.<sup>(154)</sup>

## 4. Lessons yet to be learned

The most important lesson that is yet to be learned is how to make commercial glass products which consistently display strengths exceeding ~400 MPa without the need for time and energy consuming strengthening steps. Focus on resource conservation and energy consumption with low carbon footprint process requires that commercial glass products move towards lightweighting. While the need for mechanical robustness of some products may require thick wall weight, others could greatly benefit from improved glass compositions and manufacturing processes which take advantage of reduced intrinsic flaws coupled with low hydrostatic yield strength and a high shear yield strength of the glass network to absorb handling impacts causing extrinsic flaws. Extensive research is needed in this topic. Reduced extrinsic flaws will, of course, also affect the possibilities for strengthening and coatings. For thermal strengthening, the initial intrinsic and extrinsic flaws are a determining step as to how rapidly a glass can be cooled. Chemical strengthening process time can be reduced if the extrinsic flaws are reduced, and

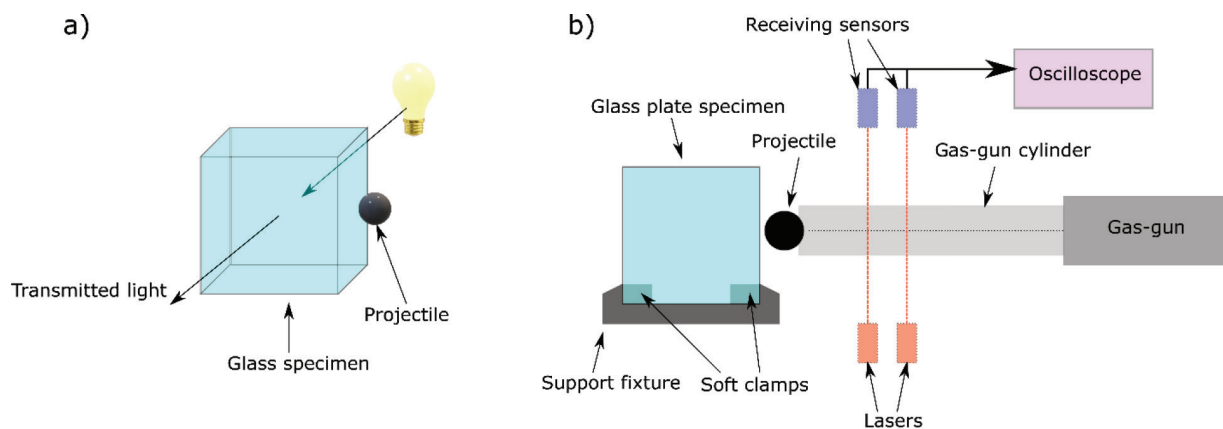


Figure 12. Edge-on impact principle and setup shown in (a) and (b), respectively [Colour available online]

coatings can possibly be made thinner which also may influence the deposition time, depending on the deposition method. Coating formulation and deposition techniques for a wider variety of glass products are other topics to be further explored. Inorganic coatings, in addition, may act as protection against sharp contact,<sup>(3)</sup> and additionally manage environmental conditions by being less prone to interact with humidity and manage applied tension by being prestressed to be in compression.

Another lesson yet to be learned is how to explore and take advantage of the possibility of nondestructive testing of glass strength.<sup>(155)</sup> It is a topic that also requires extensive research as it is a rather unexplored topic, and it will likely not replace destructive testing but be a complement.

## 5. Summary

Ordinary glass products remain brittle despite centuries of efforts to produce “flexible” or “unbreakable” glass on a commercial scale. Among the many factors that require attention are product geometry, surface flaw control, environment, introduction of surface compression, energy absorption control, and control of fracture. Thermal tempering, chemical strengthening using ion exchange, and overglazing are off-the-shelf commercial technologies which introduce surface compression and are marketed in the form of several commercial products. Thermal tempering of thin-walled products is almost ready to be brought to commercial processing. This is important towards our sustainability efforts to reduce greenhouse gases. Lamination of glass with polymers to control energy absorption and contained fracture is also used in several glass products. Research is needed to improve glass compositions that resist intrinsic as well as extrinsic flaw formation.

## Acknowledgments

SK acknowledges funding by FORMAS, the Swedish Research Council for Sustainable Development (Grant No. 2018-00707).

## References

1. Varshneya, A. K. Chemical Strengthening of Glass: Lessons Learned and Yet To Be Learned. *Int. J. Appl. Glass Sci.*, 2010, **1**(2), 131–142. DOI:10.1111/j.2041-1294.2010.00010.x
2. Varshneya, A. K. Stronger glass products: Lessons learned and yet to be learned. *Int. J. Appl. Glass Sci.*, 2018, **9**(2), 140–155. DOI:10.1111/ijag.12341
3. Varshneya, A. K., Macrelli, G., Yoshida, S., Kim, S. H., Ogrinc, A. L. & Mauro, J. C. Indentation and abrasion in glass products: Lessons learned and yet to be learned. *Int. J. Appl. Glass Sci.*, 2022, **13**(3), 308–337. DOI:10.1111/ijag.16549
4. Duran, A. & Parker, J. M. *Welcome to the Glass Age: celebrating the United Nations International Year of Glass*, CSIC, Madrid, Spain, 2022.
5. Varshneya, A. K. & Mauro, J. C. *Fundamentals of Inorganic Glasses*, Elsevier, 2019.
6. Wondraczek, L., Bouchbinder, E., Ehrlicher, A., Mauro, J. C., Sajzew, R. & Smedskjaer, M. M. Advancing the Mechanical Performance of Glasses: Perspectives and Challenges. *Adv. Mater.*, 2022, **34**(14), 2109029. DOI:10.1002/adma.202109029
7. Peter, K. W. Densification and flow phenomena of glass in indentation experiments. *J. Non-Cryst. Solids*, 1970, **5**(2), 103–115. DOI:10.1016/0022-3093(70)90188-2
8. Strabo, *Geography*, v. 8.
9. Pliny, *Naturalis Historia XXXVI*, 195, 1xvi.
10. Petronius, *Satyricon*, 66, 50,7.
11. Dio, C. *Historia Romana* 57.21.7.
12. Isidore, *Etymologiae XVI.16.6*, De Vitro.
13. Fabre, P.-J. *Palladium spagyricum Petri Ioannis Fabri doctoris medici Monspelienensis*.
14. Beretta, M. When glass matters: studies in the history of science of art from Graeco-Roman antiquity to Early Modern Era. *When glass matters*, 2004.
15. Salomon, W. *Polygraphy: Or the art of Drawing, Engraving, Etching, Limning, Painting*.
16. Neri, A. *L'arte vetraria*, 1612.
17. Lucchini, F. Aleardino's Glass. *Art Hist.*, 2013, **36**(3), 498–517. DOI:10.1111/1467-8365.12016
18. Rottländer, R. C. Naturwissenschaftliche Untersuchungen zum römischen Glas in Köln. *Kölner Jahrbuch Vor- Frühgeschichte*, 1990, **23**, 563–582.
19. Eggert, G. “Vitrum flexile” als rheinischer Bodenfund? *Kölner Jahrbuch Vor- Frühgeschichte*, 1991, **24**, 287–296.
20. Aben, H., Anton, J., Peterson, P. & Öis, M. On the Fracture Mechanics of Prince Rupert's Drops. *Cham*, 2019.
21. Aben, H., Anton, J., Öis, M., Viswanathan, K., Chandrasekar, S. & Chaudhri, M. M. On the extraordinary strength of Prince Rupert's drops. *Appl. Phys. Lett.*, 2016, **109**(23), 231903. DOI:10.1063/1.4971339
22. Hooke, R. Observation vii. of some phaenomena of glass drops. *Micrographia or Some Physiological Descriptions of Minute Bodies made by Magnifying Glasses with Observation and Inquiries thereupon*, London, 1665, 33–44.
23. Neri, A. & Merret, C. An Account of the Glass Drops. Translation of Neri's *The art of glass, wherein are shown the wayes to make and colour glass, pastes, enamels, lakes, and other curiosities with some observations on the author; whereunto is added an account of the glass drops made by the Royal Society, meeting at Gresham College*. Octavian Pulleyn, London, England, 1662, 353–362.
24. Brodsley, L., Frank, F. C., Steeds, J. W., Jones, R. V. & Paton, W. D. M. Prince Rupert's drops. *Notes Records R. Soc. London*, 1986, **41**(1), 1–26. DOI:10.1098/rsnr.1986.0001
25. Le Cat, C. N. A Memoir on the Lacrymae Batavae, or Glass-Drops, the Tempering of Steel, and Effervescence, Accounted for by the Same Principle. By Claud, Nic. le Cat, M. D. F. R. S. &c. Translated from the French, by T. S. M. D. *Phil. Trans.*, 1749, **46**, 175–188.
26. Beckmann, J., Johnston, W. & Francis, W. Prince Rupert's Drops – Lacrymae Vitreae. *History of Inventions, Discoveries and Origins*, 1846, **2**, 241–245.
27. de la Bastie, F. A New Process of Tempering Flat and Shaped Glass, and Furnaces and Machinery to Be Employed Therefor, *GB*, 2 1874.
28. Nascimento, M. L. F. & Zanotto, E. D. On the first patents, key inventions and research manuscripts about glass science and technology. *World Patent Inf.*, 2016, **47**, 54–66. DOI:10.1016/j.wpi.2016.10.002
29. Gardon, R. Thermal Tempering of Glass. *Glass Science and Technology vol 5 Elasticity and Strength in Glasses, Vol. 5*. Eds. D. R. Uhlmann & N. J. Kreidl. Academic Press, New York, 1980, 145–216.
30. Mechanic, E. Hardening and Tempering Glass. *Van Nostrand's Eclectic Eng. Mag.*, 1876, **90**(14) 511.
31. Siemens, F. Glass, tempered. *J. Soc. Arts*, 1884, **33**, 386.
32. Brookfield, J. M. Improvement in Processes of Annealing Glass, Patent No. 170,339, United States Patent Office, 1875.
33. Rogers, G. E. Improvement in Processes for Annealing Glass, Patent No. 176,066, United States Patent Office, 1876.
34. Seiden, R. A. Verfahren zur Härtung von Flachgläsern (A Process for the Curing of Flat Glass). AT 136,536, 1934.
35. Adams, L. H. & Williamson, E. D. The annealing of glass. *J. Franklin Inst.*, 1920, **190**(5), 597–631. DOI:10.1016/S0016-0032(20)90856-6
36. Bartenev, G. M. A Study of the Tempering of Glass (in Russian). *Zh. Tekhn. Fiz.*, 1949, **19**, 1423.
37. Acloque, P. Comparison Between Heat-Transfer Conditions and Setting Up of Strain in Glass During Heat-Treatment. *J. Am. Ceram. Soc.*, 1961, **44**(7), 364–373. DOI:10.1111/j.1151-2916.1961.tb15922.x
38. Narayanaswamy, O. S. & Gardon, R. Calculation of Residual Stresses in Glass. *J. Am. Ceram. Soc.*, 1969, **52**(10), 554–558. DOI:10.1111/j.1151-2916.1969.tb09163.x
39. Guillemet, C. Annealing and tempering of glass. *J. Non-Cryst. Solids*, 1990, **123**(1–3), 415–426. DOI:10.1016/0022-3093(90)90813-2

40. Gora, P., Kiefer, W., Sack, W. & Seidel, H. Thermisches Vorspannen von Spezialgläsern durch Abschrecken in Mineralölen und geschmolzenen Salzen. *Glastech. Ber.*, 1977, **50**, 319–327.
41. Winkelmann, A. & Schott, O. Ueber thermische Widerstandskoeffizienten verschiedener Gläser in ihrer Abhängigkeit von der chemischen Zusammensetzung. *Annal. Phys.*, 1894, **287**(4), 730–746. DOI:10.1002/andp.18942870407
42. Steiner, J. Otto Schott and the invention of borosilicate glass. *Glastech. Ber.*, 1993, **66**(6–7), 165–173.
43. Faraday, M. The Bakerian Lecture. On the manufacture of glass for optical purposes. *Phil. Trans. R. Soc. London*, 1830, (120) 1–57.
44. Stokes, G. G. Notices of the Researches of the Late Rev. William Vernon Harcourt. *Report of the Forty-first Meeting of the British Association for the Advancement of Science*, 1871, 38–41.
45. Kurkjian, C. R. & Prindle, W. R. Perspectives on the History of Glass Composition. *J. Am. Ceram. Soc.*, 1998, **81**(4), 795–813. DOI:10.1111/j.1151-2916.1998.tb02415.x
46. Jensen, W. B. The origin of Pyrex. *J. Chem. Ed.*, 2006, **83**(5), 692.
47. Berger, E. Über unzerbrechliches und hämmerbares Glas. *Naturwissenschaften*, 1924, **12**(4), 79–83. DOI:10.1007/BF01506347
48. Bénédictus, E. Verre armé par interposition d'une âme en celluloid. FR Patent 405,881, 1912.
49. Fullicks, A. T. British Patent 15,303, 1885.
50. Woods, J. C. British Patent 9972, 1905.
51. Watkins, G. B. & Ryan, J. D. Cellulose Acetate Plastic Improves Laminated Safety Glass. *Ind. Eng. Chem.*, 1933, **25**(11), 1192–1195.
52. Watkins, G. B. & Harkins, W. Laminated Safety Glass. *Ind. Eng. Chem.*, 1933, **25**(11), 1187–1192.
53. Zang, M. & Chen, S. Laminated glass. *Wiley Encyclopedia of Composites*, 2011, 1–7.
54. Beall, G. H. Dr. S. Donald (Don) Stookey (1915–2014): Pioneering Researcher and Adventurer. *Front. Mater.*, 2016, **3**(37). DOI:10.3389/fmats.2016.00037
55. Turner, W. E. S. The Testing of Glass Containers for Chemical Durability. *J. Am. Ceram. Soc.*, 1935, **18**(1–12) 135–141. DOI:10.1111/j.1151-2916.1935.tb19368.x
56. Boow, J. & Turner, W. E. S. The effect of annealing in a sulphur dioxide-containing atmosphere on the modulus of rupture of sheet glass. *J. Soc. Glass Technol.*, 1938, **22**, T357–T391.
57. Williams, H. S. & Weyl, W. A. Surface Dealkalization of Finished Glassware. *Glass Ind.*, 1945, **26**(6), 275–277.
58. Douglas, R. W. & Isard, J. O. The Action of Sulphur Dioxide and of Water on Glass Surfaces. *J. Soc. Glass Technol.*, 1949, **33**, T289.
59. Karlsson, S., Jonson, B. & Stålhandske, C. The technology of chemical glass strengthening - a review. *Glass Technol.: Eur. J. Glass Sci. Technol. A*, 2010, **51**(2), 41–54.
60. Kistler, S. S. Coherent expanded aerogels and jellies. *Nature*, 1931, **127**(3211), 741–741.
61. Stewart, O. J. & Young, D. W. The Action of Molten Lithium Salts on Glass. *J. Am. Chem. Soc.*, 1935, **57**(4), 695–698. DOI:10.1021/ja01307a029
62. Ernsberger, F. M. & Orowan, E. Detection of strength-impairing surface flaws in glass. *Proc. R. Soc. London. A. Math. Phys. Sci.*, 1960, **257**(1289), 213–223. DOI:10.1098/rspa.1960.0145
63. Siede, B. Etching Effect of Lithium Nitrate on Glass. *Glas Appar.*, 1937, **18**(16), 163.
64. Acoque, P. & Tochon, J. *Measurement of the Mechanical Strength of Glass after Reinforcement*, Florence, Italy, 1961.
65. Olcott, J. S. Chemical Strengthening of Glass: After more than 70 years of research, glasses can now be made strong enough to be bent sharply. *Science*, 1963, **140**(3572), 1189–1193.
66. Nordberg, M. E., Mochel, E. L., Garfinkel, H. M. & Olcott, J. S. Strengthening by Ion Exchange. *J. Am. Ceram. Soc.*, 1964, **47**(5), 215–219.
67. Shaver, W. W., Bernal, J. D., Bawn, C. E. H., Cottrell, A. H. & Frank, F. C. Some recent developments in high-strength glasses and ceramics. *Proc. R. Soc. London. A. Math. Phys. Sci.*, 1964, **282**(1388), 52–56. DOI:10.1098/rspa.1964.0212
68. Eckert, H. & Letz, M. Technical glasses. *From Construction Materials to Technical Gases*, 2022, 271.
69. Orowan, E. Fracture and strength of solids. *Rep. Progr. Phys.*, 1949, **12**(1), 185. DOI:10.1088/0034-4885/12/1/309
70. Freiman, S. W. Fracture Mechanics of Glass. *Glass Science and Technology, Vol. 5*. Eds. D. R. Uhlmann & N. J. Kreidl. Elsevier, 1980, 21–78. DOI:10.1016/B978-0-12-706705-6.50007-2
71. Ito, S. & Taniguchi, T. Effect of cooling rate on structure and mechanical behavior of glass by MD simulation. *J. Non-Cryst. Solids*, 2004, **349**, 173–179. DOI:10.1016/j.jnoncrysol.2004.08.180
72. Kurkjian, C. R., Gupta, P. K. & Brow, R. K. The Strength of Silicate Glasses: What Do We Know, What Do We Need to Know? *Int. J. Appl. Glass Sci.*, 2010, **1**(1), 27–37.
73. Ciccotti, M. Stress-corrosion mechanisms in silicate glasses. *J. Phys. D: Appl. Phys.*, 2009, **42**(21), 214006. DOI:10.1088/0022-3727/42/21/214006
74. Inglis, C. E. Stresses in a Plate due to Presence of Cracks and Sharp Corners. *Trans. R. Inst. Naval Architect.*, 1913, **55**, 219–241.
75. Griffith, A. A. The Phenomena of Rupture and Flow in Solids. *Phil. Trans. R. Soc. London A*, 1921, **221**, 163–198.
76. Irwin, G. Analysis of stresses and strains near the end of a crack traversing a plate. *J. Appl. Mech.*, 1957, **24**, 361–364.
77. Wiederhorn, S. M. Influence of Water Vapor on Crack Propagation in Soda-Lime Glass. *J. Am. Ceram. Soc.*, 1967, **50**(8), 407–414. DOI:10.1111/j.1151-2916.1967.tb15145.x
78. Pilkington, L. A. B. Review Lecture - The Float Glass Process. *Proc. R. Soc. London A, Math. Phys. Sci.*, 1969, **314**(1516), 1–25.
79. Macrelli, G., Varshneya, A. K. & Mauro, J. C. Ultra-thin glass as a substrate for flexible photonics. *Opt. Mater.*, 2020, **106**, 109994. DOI:10.1016/j.optmat.2020.109994
80. Rawson, H. & Turton, G. The Effect of Coatings in Reducing the Damage of Glass Surfaces. *Glastech. Ber.*, 1973, **46**, 28.
81. Bartenev, G. M. Theory of mechanical strengthening of glass by quenching (in Russian). *Dokl. Akad. Nauk SSSR*, 1948, **60**, 257.
82. Bartenev, G. M. The phenomenon of the hardening of glass (in Russian). *Zh. Tekh. Fiz.*, 1948, **383**–388.
83. Acoque, P. Etude experimentale de l'effet de certains traitements thermiques sur le verre et de leur influence sur les contraintes mecaniques internes. *Verres Refract.*, 1950, **4**(1), 10–19.
84. Standard Z26.1. American National Standards Institute, 1973.
85. Standard Z97.1. American National Standards Institute, 1975.
86. Narayanaswamy, O. S. Stress and Structural Relaxation in Tempering Glass. *J. Am. Ceram. Soc.*, 1978, **61**(3–4), 146–152. DOI:10.1111/j.1151-2916.1978.tb09259.x
87. Gardon, R. Variation of Densities and Refractive Indices in Tempered Glass. *J. Am. Ceram. Soc.*, 1978, **61**(3–4), 143–146. DOI:10.1111/j.1151-2916.1978.tb09258.x
88. Indenbom, V. & Vidro, L. Thermoplastic and structural stresses in solids (Residual stress in solids during heat treatment, comparing magnitudes of thermoplastic and structural stresses). *Sov. Phys. Solid State*, 1964, **6**, 767–772.
89. Aggarwala, B. & Saibel, E. Tempering stresses in an infinite glass plate. *Phys. Chem. Glasses*, 1961, **2**(5), 137–140.
90. Lee, E. H., Rogers, T. G. & Woo, T. C. Residual Stresses in a Glass Plate Cooled Symmetrically from Both Surfaces. *J. Am. Ceram. Soc.*, 1965, **48**(9), 480–487. DOI:10.1111/j.1151-2916.1965.tb14805.x
91. Carre, H. & Daudeville, L. Numerical Simulation of Soda-Lime Silicate Glass Tempering. *J. Phys. IV*, 1996, **6**(C1), 175–185.
92. Kiefer, W. & Lindig, O. Method for Thermal Prestressing of Glass. *Strength of Inorganic Glass*, Ed. C. R. Kurkjian, Plenum Press, 1985, 501–511.
93. Kiefer, W. *Thermal toughening of low-expansion glasses*, New Delhi, India, 1986.
94. Aronen, A. Doctoral Dissertation: Modelling of Deformations and Stresses in Glass Tempering. Tampere University of Technology, 2012.
95. McMaster, R. A., Shetterly, D. M. & Bueno, A. G. Annealed and tempered glass. *Engineered Materials Handbook: Ceramic and Glasses, Vol. 4*. ASM International, 1991, 453–459.
96. Mader, L. Method and device for tempering glass, US patent 9,221,708 B2. Lisec Austria GmbH, 2012.
97. Mader, L. Method and device for tempering glass, European patent EP 2,616,396 B1. Lisec Austria GmbH, 2018.
98. LISEC Aeroflat technology – Machinery for glass tempering, Technical brochure, <https://www.lisec.com/solutions/individual-machines/detail/aeroflat/aeroflat>
99. Sajzew, R. & Wondraczek, L. Thermal strengthening of low-expansion glasses and thin-walled glass products by ultra-fast heat extraction. *J. Am. Ceram. Soc.*, 2021, **104**(7), 3187–3197. DOI:10.1111/jace.17759
100. Akfirat, J. C. & Gardon, R. US Patent No. 3,694,182. Glass tempering die construction. Ford Motor Co., 1972.
101. Lezzi, P. J., Maschmeyer, R. O., Thomas, J. C. & Wasson, K. L. Thermally strengthened architectural glass and related systems and methods, US Patent 9,296,638 B2. Corning Inc., 2016.
102. Lezzi, P. J., Maschmeyer, R. O., Thomas, J. C. & Wasson, K. L. Thermally strengthened architectural glass and related systems and methods, US Patent 10,611,664 B2. Corning Inc., 2020.
103. Varshneya, A. K. The Physics of Chemical Strengthening of Glass: Room for a New View. *J. Non-Cryst. Solids*, 2010, **356**(44–49), 2289–2294. DOI:10.1016/j.jnoncrysol.2010.05.010
104. Cooper, A. R. & Krohn, D. A. Strengthening of glass fibers: II, Ion exchange. *J. Am. Ceram. Soc.*, 1969, **52**(12), 665.

105. Varshneya, A. K., Olson, G. A., Kreski, P. K. & Gupta, P. K. Buildup and relaxation of stress in chemically strengthened glass. *J. Non-Cryst. Solids*, 2015, **427**, 91–97. DOI:10.1016/j.jnoncrysol.2015.07.037
106. Gruzin, P. L. *Dokl. Akad. Nauk SSSR*, 1952, **86**(2), 289.
107. Varshneya, A. K. Kinetics of ion exchange in glasses. *J. Non-Cryst. Solids*, 1975, **19**, 355–365. DOI:10.1016/0022-3093(75)90099-X
108. Bartholomew, R. F. & Garfinkel, H. M. Chemical Strengthening of Glass. *Glass Science and Technology. Elasticity and Strength in Glasses, Vol. 5*. Eds. D. R. Uhlmann & N. J. Kreidl, Academic Press, New York, 1980, 217–270.
109. Zhang, L. & Guo, X. Thermal history and its implications: A case study for ion exchange. *J. Am. Ceram. Soc.*, 2020, **103**(7), 3971–3977. DOI:10.1111/jace.17027
110. Allan, D. C., Ellison, A. J. & Mauro, J. C. Heat treatment for strengthening glasses, US Patent 9,751,802 B2. Corning Incorporated, 2017.
111. Macrelli, G., Varshneya, A. K. & Mauro, J. C. Thermal treatment of ion-exchanged glass. *Int. J. Appl. Glass Sci.*, 2023, **14**(1), 7–17. DOI:10.1111/ijag.16590
112. Varshneya, A. K. Warp Reduction in Thin Chemically Strengthened Float Glasses. 78th Conference on Glass Problems, 2018, 191–200. DOI:10.1002/9781119519713.ch17
113. Xu, J., Zhang, B., Huo, Y. & Ma, J. Effect of Additives in Molten Salt on Ion Exchange and Strengthening of Glass. *J. Chin. Ceram. Soc.*, 2009, **37**(5), 851–854.
114. Sozanski, M. R. & Varshneya, A. K. *Am. Ceram. Soc. Bull.*, 1987, **66**(11), 1630.
115. Chinella, R. Lightweighting of Glass Containers. Proceedings of the 49th Conference on Glass Problems, *Ceram. Eng. Sci. Proc.*, 1989, 173–181. DOI:10.1002/9780470310533.ch7
116. Langille, K. B., Nguyen, D., Bernt, J. O., Veinot, D. E. & Murthy, M. K. Mechanism of dehydration and intumescence of soluble silicates: Part I Effect of silica to metal oxide molar ratio. *J. Mater. Sci.*, 1991, **26**(3), 695–703. DOI:10.1007/BF00588306
117. Wang, F., Cai, M. & Yan, L. Effect of Poly(acrylamide-acrylic acid) on the Fire Resistance and Anti-Aging Properties of Transparent Flame-Retardant Hydrogel Applied in Fireproof Glass. *Polymers*, 2021, **13**(21), 3668. DOI:10.3390/polym13213668
118. Yi, L., Zhou, L., Yan, L. & Xu, Z. Preparation of polyethylene glycol/polyacrylamide interpenetrating network hydrogel for simultaneously enhancing the fire protection and aging resistance of fireproof glass. *J. Appl. Polym. Sci.*, 2023, **140**(45), e54644. DOI:10.1002/app.54644
119. Karlsson, S., Chima, D., Varshneya, A. K., Aronen, A., Macrelli, G., Ali, S. & Mauro, J. C. Sustainable Glass Manufacturing and Lightweighting of Glass Products. *Manuscript*, (2023).
120. Alfred University Develops Stronger Glass for Use in Mobile Appliances. *Am. Ceram. Soc. Bull.*, 2008, **87**(3), 3.
121. Sehgal, J. & Ito, S. Brittleness of glass. *J. Non-Cryst. Solids*, 1999, **253**(1–3), 126–132. DOI:10.1016/S0022-3093(99)00348-8
122. Sehgal, J. & Ito, S. A New Low-Brittleness Glass in the Soda-Lime-Silica Glass Family. *J. Am. Ceram. Soc.*, 1988, **81**(9), 2485–2488. DOI:10.1111/j.1151-2916.1998.tb02649.x
123. Varshneya, A. K. Composition- and structure-dependence of brittleness in glass. *Proc. XXI Int. Congr. Glass*, Paper S1, Strasbourg, France, July 2007.
124. Mauro, J. C., Tandia, A., Vargheese, K. D., Mauro, Y. Z. & Smedskjaer, M. M. Accelerating the Design of Functional Glasses through Modeling. *Chem. Mater.*, 2016, **28**(12), 4267–4277. DOI:10.1021/acs.chemmater.6b01054
125. Matheson, H. & Skirrow, F. Vinyl ester resins and process of making same. US Patent 1,725,362.
126. Fix, E. L. Safety Glass. US Patent 2,045,130. Pittsburg Plate Glass Company, 1936.
127. Galuppi, L., Manara, G. & Royer-Carfagni, G. Practical expressions for the design of laminated glass. *Composites B: Eng.*, 2013, **45**(1), 1677–1688. DOI:10.1016/j.compositesb.2012.09.073
128. Galuppi, L. & Royer-Carfagni, G. The effective thickness of laminated glass plates. *J. Mech. Mater. Struct.*, 2012, **7**(4), 375–400. DOI:10.2140/jomms.2012.7.375
129. Galuppi, L. & Royer-Carfagni, G. F. Effective thickness of laminated glass beams: New expression via a variational approach. *Eng. Struct.*, 2012, **38**, 53–67. DOI:10.1016/j.engstruct.2011.12.039
130. Wölfel, E. Nachgiebiger verbund. eine näherungslosung und deren anwendungsmöglichkeiten. *Stahlbau*, 1987, **56**(6), 173–180.
131. Calderone, I., Davies, P. S., Bennison, S. J., Xiaokun, H. & Gang, L. Effective Laminate Thickness for the Design of Laminated Glass. Tampere, Finland, 2009.
132. Bennison, S. J., Qin, M. H. & Davies, P. S. High-performance laminated glass for structurally efficient glazing. *Innovative light-weight structures and sustainable facades*, Hong Kong, 2008.
133. Ivanov, I. V. Analysis, modelling, and optimization of laminated glasses as plane beam. *Int. J. Solids Struct.*, 2006, **43**(22), 6887–6907. DOI:10.1016/j.ijsolstr.2006.02.014
134. Aşık, M. Z. & Tezcan, S. A mathematical model for the behavior of laminated glass beams. *Comput. Struct.*, 2005, **83**(21), 1742–1753. DOI:10.1016/j.compstruc.2005.02.020
135. Norville, H. S., King, K. W. & Swoford, J. L. Behavior and Strength of Laminated Glass. *J. Eng. Mech.*, 1998, **124**(1), 46–53. DOI:10.1061/(ASCE)0733-9399(1998)124:1(46)
136. López-Aenlle, M. & Pelayo, F. Dynamic effective thickness in laminated-glass beams and plates. *Composites B: Eng.*, 2014, **67**, 332–347. DOI:10.1016/j.compositesb.2014.07.018
137. Castori, G., Pisano, G. & Speranzini, E. A theoretically-based novel protocol for the analytic treatment of the glass failure stresses associated with coaxial double ring test method. *Ceram. Int.*, 2021, **47**(14), 19784–19799. DOI:10.1016/j.ceramint.2021.03.318
138. Kim, H.-S., Yoo, B.-y., Ha, B.-K., Jeong, H.-S. & Park, S.-H. Investigation of stress fields for non-standard sized glass plates loaded by ring-on-ring. *J. Eur. Ceram. Soc.*, 2022, **42**(5), 2429–2440. DOI:10.1016/j.jeurceramsoc.2022.01.015
139. Shupikov, A. N., Ugrimov, S. V., Smetankina, N. V., Yareshchenko, V. G., Onhirsky, G. G., Ukolov, V. P., Samoilenko, V. F. & Avramenko, V. L. Bird Dummy for Investigating the Bird-Strike Resistance of Aircraft Components. *J. Aircraft*, 2013, **50**(3), 817–826. DOI:10.2514/1.C032008
140. Morse, A. L. Bird-proof windshields. *Flying Mag.*, 1943, **33**(1), 40–42.
141. Marulo, F. & Guida, M. Design criteria for birdstrike damage on windshield. *Adv. Aircraft Spacecraft Sci.*, 2014, **1**(2), 233. DOI:10.12989/aas.2014.1.2.233
142. Kahsay, B. G. & Nallamothu, R. B. Finite element analysis of bird impact with windshield of a vehicle. *Heliyon*, 2023, **9**(11), e21605. DOI:10.1016/j.heliyon.2023.e21605
143. Cannon, D. D., Musso, C. S., Williams, J. C. & Eagar, T. W. Analysis of brittle fracture of soda glass bottles under hydrostatic pressure. *J. Failure Anal. Prevent.*, 2004, **4**(5), 72–77. DOI:10.1361/15477020420800
144. Bhargava, A., Wang, F., Wood, B., Higginbotham, G. & Gentle, I. Studies of polyethylene-coated tin oxide films on glass bottles. *Surface Interface Anal.*, 2000, **29**(10), 663–670. DOI:10.1002/1096-9918(200010)29:10<663::AID-SIA919>3.0.CO;2-A
145. Hopkinson, B. X. A method of measuring the pressure produced in the detonation of high explosives or by the impact of bullets. *Philos. Trans. R. Soc. London. A. Math. Phys.*, 1914, **213**(497–508), 437–456. DOI:10.1098/rsta.1914.0010
146. Kolsky, H. An Investigation of the Mechanical Properties of Materials at very High Rates of Loading. *Proc. Phys. Soc. B*, 1949, **62**(11), 676. DOI:10.1088/0370-1301/62/11/302
147. Davies, R. M. & Taylor, G. I. A critical study of the Hopkinson pressure bar. *Philos. Trans. R. Soc. London A. Math. Phys. Sci.*, 1948, **240**(821), 375–457. DOI:10.1098/rsta.1948.0001
148. Chen, X., Wang, C., Chen, S., Yi, S. & Lu, Y. Characterization of the dynamic mechanical properties of low-iron float glass through Split-Hopkinson-Pressure-Bar tests. *Constr. Build. Mater.*, 2023, **365**, 130083. DOI:10.1016/j.conbuildmat.2022.130083
149. Kreuzer, M. Strain measurement with fiber Bragg grating sensors. *HBM, Darmstadt, S2338-1.0 e*, 12 (2006).
150. Grujicic, M., Pandurangan, B., Coutris, N., Cheeseman, B. A., Fountzoulas, C., Patel, P., Templeton, D. W. & Bishnoi, K. D. A simple ballistic material model for soda-lime glass. *Int. J. Impact Eng.*, 2009, **36**(3), 386–401. DOI:10.1016/j.ijimpeng.2008.08.001
151. Senf, H., Strassburger, E. & Rothenhäusler, H. Stress wave induced damage and fracture in impacted glasses. *J. Phys. IV*, 1994, **4**(C8), C8-741–C8-746.
152. Sheikh, M. Z., Atif, M., Raza, M. A., Suo, T., Li, Y., Zhou, F. & Dar, U. A. Damage propagation and dynamic material properties of aluminosilicate glass. *J. Non-Cryst. Solids*, 2020, **547**, 120313. DOI:10.1016/j.jnoncrysol.2020.120313
153. Hand, R. J. Mechanical Properties of Inorganic Glasses. *Encyclopedia of Glass Science, Technology, History, and Culture*, 2021, 379–390. DOI:10.1002/9781118801017.ch3.11
154. Hand, R. J., Varner, J., Nattermann, K. & Müller-Simon, H. Strength of Glass Basics and Test Procedures, ICG Advanced Course, Deutsche Glastechnischen Gesellschaft, 2006.
155. Karlsson, S., Kozłowski, M., Grund, L., Andersson, S. A. K., Haller, K. C. E. & Persson, K. Non-destructive strength testing of microindented float glass by a nonlinear acoustic method. *Constr. Build. Mater.*, 2023, **391**, 131748. DOI:10.1016/j.conbuildmat.2023.131748